UNIVERSITY FOR DEVELOPMENT STUDIES

INVESTIGATIONS INTO MAGNETOHYDRODYNAMIC BOUNDARY LAYER FLOW PAST INCLINED SURFACES

AYINE AZURE DANIEL

2015

UNIVERSITY FOR DEVELOPMENT STUDIES

INVESTIGATIONS INTO MHD BOUNDARY LAYER FLOW PAST INCLINED SURFACES

BY

AYINE AZURE DANIEL (B.Sc. Mathematics)

(UDS/MM/0018/13)

DISSERTATION SUBMITTED TO THE DEPARTMENT OF MATHEMATICS, FACULTY OF MATHEMATICAL SCIENCES, UNIVERSITY FOR DEVELOPMENT STUDIES, IN PARTIAL FULFILMENT OF THE REQUIREMENTS FOR THE **AWARD OF MASTER OF SCIENCE DEGREE IN MATHEMATICS**

JULY, 2015

DECLARATION

Student

I hereby declare that this dissertation is the result of my own original work and that no part of it has been presented for another degree in this university or elsewhere:

Candidate's Signature..Date...30 – 10 – 2015..

Name: **Ayine Azure Daniel.**

Supervisors'

I hereby declare that the preparation and presentation of the dissertation was supervised in accordance with the guidelines on supervision of dissertation laid down by the University for Development Studies.

Supervisor's Signature..Date...01/11/2015..

Name: **Ing. Dr. Seini Yakubu Ibrahim.**

ABSTRACT

This dissertation investigates the effect of heat and mass transfer over a heated inclined plate with viscous dissipation. An incompressible ferrofluid such as polyethylene oxide solution is made to uniformly flow over a heated plate and a transverse magnetic field applied to regulate the flow. The partial differential equations modelling the problem include the continuity, momentum, energy and concentration equations. The resulting system of partial differential equations is transformed into a system of non-linear ordinary differential equations by employing the technique of Similarity Analysis. The dimensionless system of third order ordinary differential equations is then transformed into a system of first order differential equations. The transformed system of first order equations is then solved by using the fourth order Runge Kutta algorithm along with shooting method, with the aid of Maple 16 computer software package. It was observed that the temperature of the plate decreased when the angle of inclination ($\propto$) increased from 0^o to 10^o ("cooling angle") and increased when the angle of inclination was greater than 10^o. The temperature also decreased when both thermal and solutal Grashof numbers (Gr) and (Gc) respectively were increased. However a rise in temperature was observed when the Prandtl number (Pr), Eckert number (Ec), Biot number (Bi), viscous dissipation parameter (N), Schmidt number (Sc) and local heat generation Parameter (Q) were increased.

ACKNOWLEDGEMENT

My profound gratitude goes to the authorities of the University for Development Studies, especially to the Department of Mathematics for the immense support given me to facilitate the execution of this work.

I am highly indebted to my supervisor, Ing. Dr. Ibrahim Yakubu Seini, who guided and supervised my work to a successful end, I very much appreciate his mentorship. My regards goes to all lecturers who shared their knowledge with me, their contribution to imparting knowledge to me is much appreciated. The research would have been impossible without the knowledge I acquired from them.

I am grateful to Mr. Atwire John Christian; I do much appreciate the enormous support he gave me whenever I needed it. I am also grateful to my uncles; Mr. Alfred Akuribila and Mr. Alfred Anafo for their support and counselling which gave me courage to come this far.

My regard also goes to my wife, Baa Mansoba Felicia for working hard to keep the family when I was busy pursuing the programme. I also appreciate the company of my classmates Timothy, Osman, Peter and Kalid throughout the programme.

My regard finally goes to all persons who have directly or indirectly contributed to the successful execution of this work.

DEDICATION

This dissertation is dedicated to my parents Mr. Ayine and Madam Lardi as well as my uncle Mr. Ayinmolga for the enormous support they gave me throughout my educational career.

TABLE OF CONTENT

CHAPTER TWO

2.0 LITERATURE REVIEW

CHAPTER THREE

CHAPTER FOUR

4.0 RESULTS AND DISCUSSIONS

CHAPTER FIVE

5.0 CONCLUSIONS AND RECOMMENDATIONS

LIST OF TABLES

LIST OF FIGURES

NOMENCLATURE

u, v, w: Velocity components along the x, y and $z-$axis directions, respectively

g: Acceleration due to gravity

ρ: Fluid density

Q_O: Heat source parameter

μ: Dynamic viscosity

ν: Kinematic viscosity

h_f: Heat transfer coefficient

T: Temperature

T_f: Temperature of hot fluid

T_∞: Temperature of fluid far away from the plate

U_∞: Velocity of fluid far away from the plate

C: Concentration

C_w: Plate surface concentration

C_∞: Free stream concentration

β_T: Thermal expansion coefficient

β_C: Concentration expansion coefficient

D: Mass diffusivity

α_o: Thermal diffusivity

κ: Thermal conductivity

M: Local Magnetic field parameter

B_o: Magnetic field strength

Gr :	Local thermal Grashof number
Gc :	Local solutal Grashof number
β :	Chemical reaction parameter
Q :	Local heat source parameter
N :	Viscous dissipation parameter
α :	Angle of inclination
$\Pr$:	Prandtl number
Sc :	Schmidt number
Ec :	Eckert number
Bi :	Local convective heat transfer parameter
σ :	Fluid electrical conductivity
δ :	Porosity parameter
η :	Similarity variable
f :	Dimensionless velocity
θ :	Dimensionless Temperature
ϕ :	Dimensionless concentration

CHAPTER ONE

1.0 INTRODUCTION

1.1 Background of the Study

Heat and mass transfer is commonly encountered in many engineering and industrial processes. Efforts to understand and control the process to achieve quality products have led to the use of various techniques. The use of magnets in flow processes have recently been known and referred to as Magnetohydrodynamics (MHD). It enables the cooling process to be controlled to achieve a desired product quality. It is important to understand the various techniques employed that have the potential of meeting this goal. This chapter presents the background, objectives and justification of the study.

Conventional base fluids such as water, air and oil have been known and used for cooling mechanical systems in industrial processes over many centuries. In recent times, the concepts of boundary layer have assumed an important dimension due to its numerous applications in engineering innovations and industrial processes. An essential part of boundary layer theory is the determination of friction drag of bodies in a flow.

(Prandtl, 1904), introduced the boundary layer theory to study the flow structure of viscous fluid near solid boundaries. The early contributions in this area of fluid dynamics include that of (Blasius, 1908), who solved the famous boundary layer equation for a flat moving plate problem and found a power series solution of the model.

(Falkner & Skan, 1931), generalized the Blaius problem by considering the boundary layer flow over a wedge inclined at a certain angle.

(Sakiadis, 1961) investigated the boundary layer flow over a continuously moving rigid surface with constant speed whilst (Crane, 1970) was the first to investigate the boundary layer flow due to a stretching surface and found exact solutions of the boundary layer equations. A numerical solution of the classical Blasius flow problem was presented by (Cortell, 2005). (Cortell, 2008), further provided numerical solutions for the Sakiadis flow by considering the effects of radiation on the boundary layer problem. The boundary layer flow characteristics of fluids in porous media have been studied extensively because of its many engineering applications such as in the design of heat exchangers, catalytic reactors, cooling devices, and during chemical reaction processes.

1.2 Problem Statement

Base fluids (water and air) have been known and used for cooling purposes in everyday life. However, they are found to be less efficient in cooling mechanical systems in industry. It has been established that the rate of cooling of a surface depends on the viscosity of the fluid and the rate at which the surface transfers the heat in the process of cooling.

The advent of ferrofluids (e.g. polyethylene oxide solution), which have both electrical and magnetic properties makes it possible to control flow kinematics with the ultimate aim of increasing the efficiency of heat transfer. The orientation of a surface is also a significant factor in determining the speed of fluid flow as it enhances the rate of heat and mass transfer over the surface. Many fluid flow processes over flat and vertical surfaces have been studied and used for cooling purposes in industry. However, to improve the efficiency of systems and quality of products, more researches is needed. An inclined surface can be considered as an obvious problem that will hasten the velocity of flow but what would that mean to the cooling process? These are issues this study will look into.

1.3 Objectives of the Study

1.3.1 General Objective

The general objective is to investigate the heat and mass transfer characteristics in MHD boundary layer flow over an inclined surface.

1.3.2 Specific Objectives

The specific objectives of the study are:

i. To develop theoretical framework modelling the flow of ferrofluid on inclined surface.

ii. To use the techniques of similarity analysis to transform the resulting partial differential equations into ordinary differential equations.

iii. To employ numerical analysis to solve the resulting boundary value problem.

iv. To analyse the effects of various controlling parameters on the rate of heat and mass transfers of ferrofluids on inclined surfaces.

1.4 Justification of Study

Many industrial processes involve the transfer of heat by means of flowing fluids to achieve cooling. The flows of ferro-fluids over inclined surfaces possess greater potential of enhancing efficient cooling. When ferro-fluids are made to flow over inclined surfaces in the presence of transverse magnetic fields, a better cooling with greater efficiency is achieved due to the fact that the flow can be regulated. This is useful in the building of small heat transfer systems with lower capital cost with improved efficiency. This study will greatly enhance the efficient cooling processes encountered in various industries such as in the electronic, medical, food processing and manufacturing industries as well as in nuclear industry.

1.5 Computational Approach

The hydromagnetic boundary layer flow over an inclined surface will be modelled in the form of differential equations, which constitute a nonlinear boundary value problem. . Nonlinear differential equations have been used extensively in describing flow processes and their solutions remain extremely important and of practical relevance. Approximate solutions for the nonlinear systems of differential equations modelling MHD flow over an inclined surface will be constructed using the fourth order Runge-Kutta integration scheme coupled with a numerical shooting technique. Results will be presented numerically and graphically and discussed quantitatively with respect to various parameters embedded in the study.

1.6 Organization of the Study

The rest of the study is organised as follows: Chapter two presents the literature review of the study with some important definitions relevant to the study. Chapter three outlines the procedure of modelling the problem in the form of differential equations. Chapter four then discusses the results of the study highlighting the effects of various controlling thermo-physical parameters. Chapter five concludes the study with some recommendations for further studies.

CHAPTER TWO

2.0 LITERATURE REVIEW

2.1 Introduction

This chapter examines existing works related to the problem under study. Review of flow on various surface orientations and chemical reactive flows together with relevant definitions of terms and concepts related to the study are presented.

2.2 Flow on various Orientations of Surfaces

Research on heat and mass transfers in fluids on different orientations has been conducted. The effect of transpiration (suction or blowing) on ordinary fluid flow and heat transfer as well as skin friction coefficients for the steady, laminar and free convection boundary layer flow over a heated horizontal surface has been studied extensively by (Hossain & Mojumder, 2010). They observed that increasing the magnitude of suction/blowing the magnitude of the velocity increases, where as with the increase of the suction and blowing the maximum values of the temperature decreases. (Gnaneswara & Bhaskar, 2011) investigated the mass transfer and heat generation effects on MHD free convection flow past an inclined vertical surface in a porous and observed that a positive increase in Eckert number reduces the velocity and temperatures in the flow. (Sivasankaran *et al.*, 2006) employed the lie group analysis method to study the natural convection heat and mass transfer in an inclined surface, and observed that the temperature and velocity of the fluid decrease at a very fast rate in the case of water in comparison with air. Increasing the Prandtl number decreases the temperature and velocity of the fluid and increases the concentration. Whilst (Ibrahim & Makinde, 2011) conducted a theoretical study of steady MHD boundary layer flow past a low-heat-resistant sheet moving vertically downwards and observed that the buoyancy force parameter increases the velocity of flow but reduces the temperature due to convective cooling.

Heat and mass transfer characteristics of natural convection of a chemically reacting Newtonian fluid along a vertical and inclined plates in the presence of diffusion-thermo (Dufour) and thermal-diffusion (Soret) effects has been studied by (Beg *et al.*, 2009). They observed that an increase in Dufour number (Du) and simultaneous decrease in Soret number (Sr) causes a rise in fluid temperature (θ). The presence of chemical reaction and non-uniform heat source over an unsteady stretching surface was investigated by (Seini, 2013), who observed that the heat and mass transfer rates as well as the skin friction coefficient depended on the unsteadiness parameter, the space-dependent and the temperature-dependent parameters for a heat source or sink.

The velocity and heat transfer in a boundary layer flow with thermal radiation past a moving vertical porous plate was examined by (Makinde *et al.,* 2007). They observed that the fluid temperature decreased with an increase in fluid suction at the plate. An increase in the fluid velocity is observed with an increase in the radiative heat absorption parameter. (Reddy *et al.,* 2010) analyzed the steady two-dimensional MHD free convection flow of viscous dissipating past a semi-infinite moving vertical plate in a porous medium with Soret and Dufour effects. They observed that a positive increase in Eckert number is shown to reduce the velocity and temperatures in the flow. Also increasing the Prandtl number substantially decreases the translational velocity and the temperature. Heat and mass transfer over a stretching sheet under the influence of a uniform transverse magnetic field and Hall current were conducted by (Shit, 2009). He observed that the flow velocities f ′ and f gradually increases with the increase of Hall current parameter m while, in the case of cross flow velocity g, temperature as well as the concentration a reversal trend was observed.

(Mansour *et al.*, 2007), analytically studied the MHD flow of a micro polar fluid due to heat and mass transfer through a porous medium bounded by an infinite vertical porous plate in the presence of a transverse magnetic field in slip-flow regime. They observed that as the magnetic parameter increase the velocity profiles decreases, the angular velocity profiles decreases and it has no effect on temperature and concentrations. Similarly, the transient free convective flow of a viscous incompressible fluid over an infinite vertical porous plate embedded in highly porous medium of time dependent permeability under periodic suction has been studied by (Ahmed, 2010). He found that the velocity of the flow field falls more rapidly for frequency of oscillation in comparison to time and all the branches of u diminishing monotonically in case of heating of the plate.

(Gnaneswara *et al.*, 2011), investigated the mass transfer and heat generation effects on MHD free convection flow past an inclined surface in a porous medium. They observed that, the boundary layer thickness decreases with an increase in the magnetic parameter.

(Aziz, 2009), obtained a similarity solution for laminar thermal boundary layer over a flat plate with a convective surface boundary condition. The paper demonstrates that a similarity solution is possible if the convective heat transfer associated with the hot fluid on the lower surface of the plate is proportional to $x^{-1/2}$. (Gebharat, 1962), examined the influence of viscous dissipation effect in natural convective flows showing that the heat transfer rates are reduced by increasing dissipation parameters.

2.3 Chemically Reactive Flows

There are many transfer processes governed by the combined action of buoyancy forces due to both thermal and mass diffusion in the presence of chemical reaction. They have many applications in nuclear reactor technology, combustion, solar collectors, drying, dehydration, polymer production and in operations of chemical and food processing plants.

The effect of chemical reaction on a moving isothermal vertical surface with suction has been investigated by (Muthucumaraswamy, 2002). He observed the velocity and concentration increased during the generative reaction and decrease in the destructive reaction. (Kandasamy, 2005), then analyzed the effects of chemical reaction and thermal stratification over vertical stretching surfaces and observed that, the flow field is influenced appreciably by the presence of thermal stratification, chemical reaction and magnetic field. The application of chemical reaction to a micropolar flow over an isothermal vertical cone has been studied by (Abdou, 2007). He found out that The influence of chemical reaction on the fluid flow along the wall of the cone accelerate with increase of chemical reaction parameter, on the other hand, temperature of the fluid increases with increase of chemical reaction parameter but concentration of the fluid reduces.

(Ibrahim *et al.*, 2008), investigated the chemical reaction and absorption effects on the unsteady MHD flow past a semi-infinite vertical permeable moving plate. They observed that, there was a fall in velocity with increase of Heat absorption parameter φ or chemical reaction parameter k or Schmidt number Sc. (Muthucumaraswamy & Janakiraman, 2008) investigated the mass transfer effect on isothermal vertical oscillating plate in the presence of chemical reaction and observed that, the concentration increases with decreasing chemical reaction parameter K and the Schmidt number Sc.

The effect of chemical reaction on free convection flow through a porous medium bounded by a vertical surface was reported by (Das, 2010). It was observed that the rate of heat transfer at the surface increased when the chemical reaction parameter increases.

(Ibrahim & Makinde, 2010), studied the effects of chemical reaction on MHD boundary layer flow of heat and mass transfer over a moving vertical plate with suction using the Newton–Raphson shooting method alongside the fourth-order Runge–Kutta integration scheme. They observed that the momentum boundary layer thickness decreased while both thermal and concentration boundary layer thicknesses increased with increasing magnetic field intensity. They concluded that increasing wall suction enhances the boundary layer thickness and reduces the skin friction together with the heat and mass transfer rate at the moving plate surface.

Etwire and seini (2014) investigated the radiative MHD flow over a vertical plate with convective boundary conditions using the fourth-order Runge-Kutta integration scheme with the shooting method and observed that the radiation parameter increases the thermal boundary layer thickness. Senapati (2012) also noticed that the mass concentration decreases when the reaction rate parameter is increased.

2.4 Basic Properties and Definitions of Terms

2.4.1 Newton's Law of Viscosity and Newtonian Fluids

According to Newton's law of viscosity for laminar flow, the shear stress is directly proportional to the strain rate or the velocity gradient; that is

$$\tau_{xy} = \mu \frac{\partial u}{\partial y}, \tag{2.1}$$

where τ_{xy} is the shear stress, μ is the constant of proportionality representing the dynamic viscosity of the fluid and $\frac{\partial u}{\partial y}$ is the velocity gradient. The shear stress is maximum at the surface of the plate in direct contact with the fluid, due to the no slip condition. Fluids obeying the Newton's law of viscosity (2.1) are referred to as Newtonian fluids. Otherwise, they are non-Newtonian

2.4.2 Fourier's Law of Heat Conduction

The Fourier's law of heat conduction relates the heat flow with temperature differences and conductivity of the medium. Assuming that, the temperature T varies directly in a direction, x it can be written mathematically as:

$$q = -k \frac{dT}{dx}, \tag{2.2}$$

where q is the heat energy through a unit area in a unit time, k is the material transport property, called the conductivity of the medium. Equation (2.2) is valid for all common solids, liquids and gases. The minus sign signify that heat flow is positive in the direction of decreasing temperature.

2.4.3 Fick's Law of Mass Diffusion

Consider a mixture of two fluid species A and B, with ρ_A and ρ_B densities respectively and suppose that ρ_A varies as ρ_B in the direction, x. Then, there will be a diffusion mass transfer of species A in the direction of its decreasing density defined by the following equation:

$$J_{AX} = -D_{AB}\frac{d\rho_A}{dx}, \tag{2.3}$$

where J_{AX} is the mass flux of species A in the direction of x and D_{AB} is the molecular diffusion coefficient, which varies with temperature, pressure and the mixture composition.

2.5 Dimensionless Parameters in Convective Heat and Mass Transfer

Dimensionless numbers measure the relative importance of different forces or the transport phenomenon involving fluid flow. In these dimensionless numbers, different properties of the flow are lumped together to represent their cumulative effect.

2.5.1 The Eckert Number (Ec)

The Eckert number (Ec) is a useful dimensionless quantity in fluid dynamics. It is the ratio of the kinetic energy to the enthalpy (or the dynamic temperature to the temperature) driving force for heat transfer and is given by:

$$Ec = \frac{u}{C_p \Delta T} \tag{2.4}$$

where u is the fluid velocity , C_p is the specific heat at constant pressure and ΔT is the driving force for heat transfer (i.e. wall temperature minus free stream temperature). The Eckert number is a key parameter in determining the viscous dissipation of energy in a low speed flow.

2.5.2 The Grashof Number (Gr)

The Grashof number is a dimensionless quantity for analysing the velocity distribution in free convection systems. It is defined as the ratio of the buoyancy force to the viscous force. The Grashof number is analogous to the Reynolds number in forced convection and given by:

$$Gr = \frac{\beta \Delta T g L^3 \rho^2}{\mu^2}, \tag{2.5}$$

where β is the volumetric expansion coefficient, ρ is the density evaluated at the mean temperature, g is the gravitational constant, ΔT is the temperature difference, L is the distance between the high temperature and low temperature regions and μ is the dynamic viscosity of the convective fluid.

2.5.3 The Prandtl Number (Pr)

The Prandtl number is defined as the ratio of viscous diffusivity to the thermal diffusivity

$$\Pr = \frac{\mu C_p}{k} \tag{2.6}$$

In heat transfer problems, the Prandtl number controls the relative thickness of the momentum and thermal boundary layers. When Pr is small, heat diffuses very quickly compared to the velocity (momentum). When both the thermal and viscous diffusivities are equal, the Prandtl number becomes unity; in which case, both the momentum and thermal boundary layers are equal.

2.5.4 The Schmidt Number (Sc)

The Schmidt number is defined as the ratio of the kinematic viscosity to the molecular diffusivity.

$$Sc = \frac{\upsilon}{D}, \tag{2.7}$$

Where D is the molecular or chemical diffusivity and υ is the kinematic viscosity or viscous diffusivity.

2.5.5 Skin Friction Co-efficient (C_f)

The dimensionless shear stress at the surface is called the skin friction coefficient given by:

$$C_f = \frac{\tau_w}{\rho\mu^2}, \tag{2.8}$$

where τ_w is the wall shear stress, ρ is the density and μ is the coefficient of dynamic viscosity. The overall skin friction coefficient, $\overline{C_f}$ is based on the average of the ratio of shear stress τ_w and the length L of the plate.

2.5.6 The Nusselt Number (Nu)

The Nusselt Number is the measure of the ratio of the magnitude of convective heat transfer rate to the magnitude of the heat transfer rate that would exist under pure conduction.

$$Nu = \frac{h_f(T_w - T)}{k(T_w - T)/l} \tag{2.9}$$

The convective heat transfer from the surface depends on the magnitude of the term $h_f(T_w - T)$, where h_f is the heat transfer coefficient and T_w and T are the temperatures of wall and fluid respectively. In the absence of flow, the heat transfer will purely be due to conduction. The Fourier's law states that the quantity $k(T_w - T)/l$ is the measure of the heat transfer rate, where k is the thermal conductivity and l is the characteristic length.

2.5.7 The Sherwood Number (Sh)

The Sherwood number (Sh) is defined as the dimensionless mass flux at the surface given as;

$$Sh = \frac{m_w x}{D(T - T_\infty)}, \tag{2.10}$$

where m_w is the mass flux at the surface and D is the diffusion coefficient.

2.5.8 The Biot Number (Bi)

The Biot number is defined as the ratio of temperature gradient within the body to the overall temperature gradient in the fluid. It is similar to the Nusselt number and given by the expression;

$$Bi = \frac{hL}{k}, \tag{2.11}$$

Were L is the characteristic length h is the heat transfer coefficient.

CHAPTER THREE

3.0 DEVELOPMENT OF MATHEMATICAL MODELS FOR FLOW PROBLEMS

3.1 Introduction

This chapter presents the mathematical derivations of equations of mass conservation, momentum, energy and concentration necessary to study all fluid flow problems.

Computational fluid dynamics is best described in the form of partial differential equations as the characteristics of flowing fluids depend on multiple flow quantities such as the distances and velocities. Hence the generalized governing equations are developed and applied to analyse a typical industrial problem. The equations are derived based on some fundamental laws of physics. The control volume approach to flow analysis is used in this study.

3.2 The Principles of Mass Conservation

Consider a parcel of fluid flowing into and out of a three dimensional infinitesimal control volume depicted in Figure 3.1.

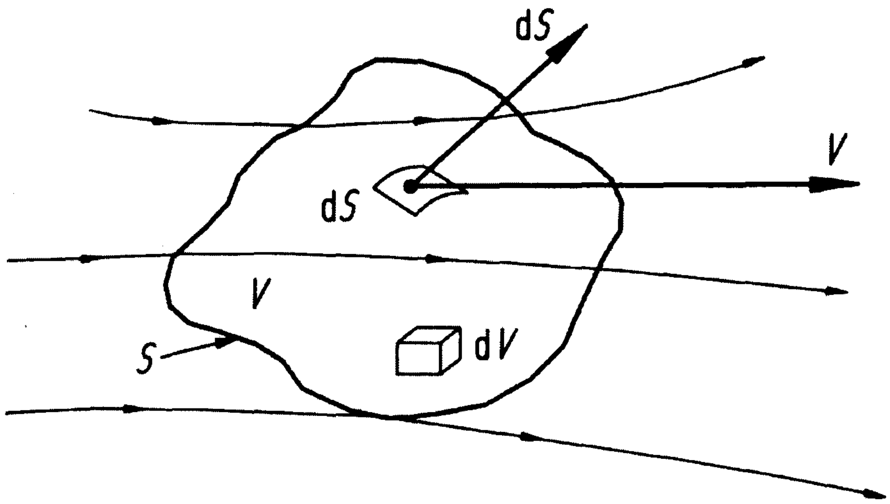

Figure 3.1: Finite control volume of moving fluid element.

At any specific time t, the control volume can be viewed as a system. The mass conservation for this infinitesimal system will be zero. That is,

$$\frac{D}{Dt}\int_V \rho dV = 0 \tag{3.1}$$

Using Reynold's Transport Theorem (RTT), equation (3.1) can be written as

$$\frac{D}{Dt}\int_V \rho dV = \frac{d}{dt}\int_V \rho dV + \int_A U_{rn}\rho dA = 0 \tag{3.2}$$

For a constant control volume, the derivative can enter into the integral on the right hand side of equation (3.2) to obtain;

$$\int_V \frac{d\rho}{dt} dV + \int U_{rn}\rho dA = 0 \tag{3.3}$$

The first term in (3.3) for the infinitesimal volume, neglecting higher order derivatives , is expressed as;

$$\int_V \frac{d\rho}{dt} dV = \frac{d\rho}{dt} dxdydz + \ldots \tag{3.4}$$

The second term in equation (3.3) is expressed as;

$$\begin{aligned}\int_A U_{rn} \rho dA = [(\rho u)|_x - (\rho u)|_{x+dx}]dydz + [(\rho v)|_y - (\rho v)|_{y+dy}]dxdz \\ + [(\rho w)|_z - (\rho w)|_{z+dz}]dxdy\end{aligned} \tag{3.5}$$

The difference between point x and $x + dx$ can be obtained by developing a Taylor series as;

$$(\rho u)|_{x+dx} = (\rho u)|_x + \left.\frac{\partial(\rho u)}{\partial x}\right|_x dx \tag{3.6}$$

It can be noticed that the operation in the x coordinate produces an additional term. The same can be done for y and z coordinates. Thus, an infinitesimal volume element dV is obtained for all directions. The result obtained by substituting (3.6) into (3.5) is divided by $dxdydz$ and simplified using the definition of the partial derivative in the regular process to obtain;

$$\int_A U_{rn} \rho dA = -\left[\frac{\partial(\rho u)}{\partial x} + \frac{\partial(\rho v)}{\partial y} + \frac{\partial(\rho w)}{\partial z}\right]$$

Combining the result obtained in simplifying the first term (3.4) and the second term, we obtained the general continuity equation in Cartesian coordinates as;

$$\frac{\partial\rho}{\partial t} + \frac{\partial\rho u}{\partial x} + \frac{\partial\rho v}{\partial y} + \frac{\partial\rho w}{\partial z} = 0 \tag{3.7}$$

For steady incompressible fluid flow, the continuity equation is simply written as;

$$\nabla \cdot U = \frac{\partial u}{\partial x} + \frac{\partial v}{\partial y} + \frac{\partial w}{\partial z} = 0, \tag{3.8}$$

where U, denotes velocities in the x, y and z directions.

3.3 The Law of Momentum Conservation

Newton's second law of motions is applicable to a small infinitesimal moving fluid. That is, the rate of change of momentum of fluid leaving a control volume is directly proportional to the sum of the forces acting on the control volume, leading to:

$$\vec{F} = m\vec{a} \tag{3.9}$$

where $\vec{F}$ the force acting on the control volume, m mass of fluid and $\vec{a}$ acceleration. One directional vector equation for the x coordinate axis is derived and generalized for the entire Cartesian system using the elemental control volume of sides dx, dy and dz shown in Figure 3.2.

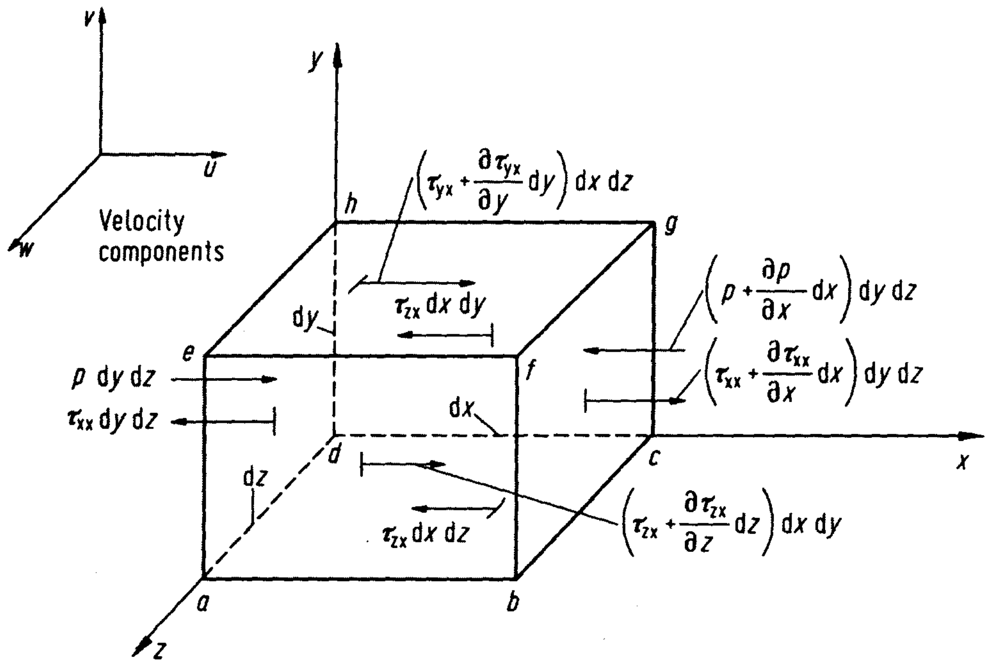

Figure 3.2: Infinitesimally small moving fluid element.

Forces acting on the cubic element of fluid include the surface forces, gravitational forces (body force) and internal forces. Only the forces in the x – direction are shown in Figure 3.2. Thus,

Internal force = Surface forces + Body forces.

Let the body force per unit mass acting on the fluid element be denoted by f_B with f_x as its x-component, the body force acting on the infinitesimal cube in the x direction is;

$$\hat{i} \cdot f_{Bx} = \rho f_x dxdydz \tag{3.10}$$

The dot product yields a force in the direction of x.

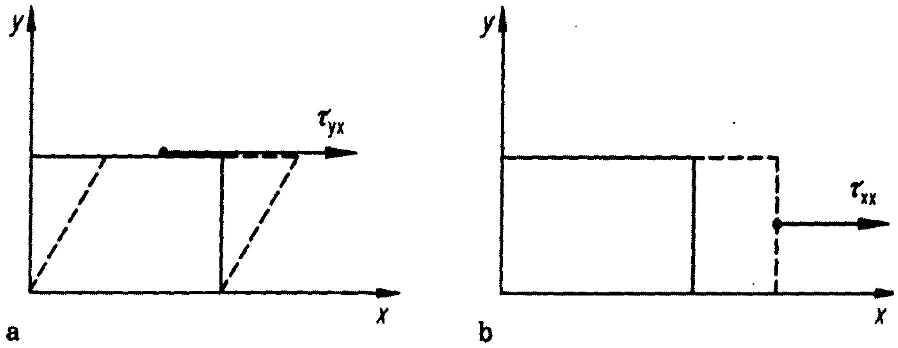

Figure 3.3: Illustration of shear stress *a* and normal stress *b*.

The surface force f_{xx} in the x direction on the x plane is;

$$f_{xx} = \tau_{xx}\big|_{x+dx} \times dydz - \tau_{xx}\big|_{x} \times dydz \tag{3.11a}$$

The surface force f_{xy} in the x direction by the y plane is;

$$f_{xy} = \tau_{yx}\big|_{y+dy} \times dxdz - \tau_{yx}\big|_{y} \times dxdz \tag{3.11b}$$

The surface force f_{xz} in the x direction by the z plane is;

$$f_{xz} = \tau_{zx}\big|_{z+dz} \times dxdy - \tau_{zx}\big|_{z} \times dxdy \tag{3.11c}$$

The pressure force f_{px} acts inwards producing a resultant in the negative x direction;

$$f_{px} = P\big|_{x} - P\big|_{x+dx} \times dydz \tag{3.11d}$$

Hence, the total net surface forces W_x resulting from pressure force shear stresses in the x direction is;

$$W_x = \left[P - \left(P + \frac{\partial P}{\partial x}dx\right)\right]dydz + \left[\left(\tau_{xx} + \frac{\partial \tau_{xx}}{\partial x}dx\right) - \tau_{xx}\right]dydz +$$

$$\left[\left(\tau_{yx} + \frac{\partial \tau_{yx}}{\partial y}dy\right) - \tau_{yx}\right]dxdz + \left[\left(\tau_{zx} + \frac{\partial \tau_{zx}}{\partial z}dz\right) - \tau_{zx}\right]dxdy$$

Simplifying yields;

$$W_x = \left(-\frac{\partial P}{\partial x} + \frac{\partial \tau_{xx}}{\partial x} + \frac{\partial \tau_{yx}}{\partial y} + \frac{\partial \tau_{zx}}{\partial z}\right)dxdydz \tag{3.12}$$

The total force in the x – direction F_x is obtained by summing equations 3.10 and 3.12;

$$F_x = \left(-\frac{\partial P}{\partial x} + \frac{\partial \tau_{xx}}{\partial x} + \frac{\partial \tau_{yx}}{\partial y} + \frac{\partial \tau_{zx}}{\partial z}\right)dxdydz + \rho f_x dxdydz \tag{3.13}$$

Equation 3.13 represents the left-hand side of equation 3.9. Considering the right-hand side of the equation, since mass of the fluid element is fixed, we have;

$$dm = \rho dxdydz$$

The acceleration of the fluid element is the time-rate-of-change of its velocity. Hence, the component of acceleration a_x in the x- direction is denoted by;

$$a_x = \frac{Du}{Dt}$$

When equations 3. 10, 3.12 and 3.13 are substituted into 3.9 the results become;

$$\frac{Du}{Dt}\rho dxdydz = \left(-\frac{\partial P}{\partial x} + \frac{\partial \tau_{xx}}{\partial x} + \frac{\partial \tau_{yx}}{\partial y} + \frac{\partial \tau_{zx}}{\partial z}\right)dxdydz + \rho f_x dxdydz$$

Simplifying yields;

$$\rho\frac{Du}{Dt}=\left(-\frac{\partial P}{\partial x}+\frac{\partial\tau_{xx}}{\partial x}+\frac{\partial\tau_{yx}}{\partial y}+\frac{\partial\tau_{zx}}{\partial z}\right)+\rho f_x \quad (2.14)$$

This is the non-conservative form of the differential momentum equation of a viscous flow in the x direction. Similarly, in the y and z directions, we have respectively;

$$\rho\frac{Dv}{Dt}=\left(-\frac{\partial P}{\partial x}+\frac{\partial\tau_{xy}}{\partial x}+\frac{\partial\tau_{yy}}{\partial y}+\frac{\partial\tau_{zy}}{\partial z}\right)+\rho f_y \quad (3.15)$$

$$\rho\frac{Dw}{Dt}=\left(-\frac{\partial P}{\partial x}+\frac{\partial\tau_{xz}}{\partial x}+\frac{\partial\tau_{yz}}{\partial y}+\frac{\partial\tau_{zz}}{\partial z}\right)+\rho f_z \quad (3.16)$$

Equations 3.14, 3.15 and 3.16 require that the stress tensor be defined in terms of velocity deformation. The relationship between the stress tensor and deformation depends on the class of materials involved. Additionally, the deformation can be viewed as a function of the velocity field. Furthermore, reduction of shear stress does not return the fluid to its original state as in some solids. However increasing the shear stress yields larger deformation. The momentum conservation equations are also called the Navier-Stokes equations. From equation 3.14, the substantial derivative can be written as;

$$\rho\frac{Du}{Dt}=\rho\frac{\partial u}{\partial t}+\rho\vec{V}\cdot\nabla u \quad (3.17)$$

That is; $\frac{\partial(\rho u)}{\partial t}=\rho\frac{\partial u}{\partial t}+u\frac{\partial\rho}{\partial t}$

Thus, $\rho\frac{\partial u}{\partial t}=\frac{\partial(\rho u)}{\partial t}-u\frac{\partial\rho}{\partial t}$ (3.18)

Applying the vector identity for the divergence of the product of a scalar times a vector, we have;

$$\nabla \cdot \left(\rho u \vec{V}\right) = u \nabla \cdot \left(\rho \vec{V}\right) + \left(\rho \vec{V}\right) \cdot \nabla u$$

Implying that;

$$\rho \vec{V} \cdot \nabla u = \nabla \cdot \left(\rho u \vec{V}\right) - u \nabla \cdot \left(\rho \vec{V}\right) \tag{3.19}$$

Substituting equations 3.18 and 3.19 into 3.17 results in;

$$\rho \frac{Du}{Dt} = \frac{\partial(\rho u)}{\partial t} - u \frac{\partial \rho}{\partial t} - u \nabla \cdot \left(\rho \vec{V}\right) + \nabla \cdot \left(\rho u \vec{V}\right)$$

This implies that;

$$\rho \frac{Du}{Dt} = \frac{\partial(\rho u)}{\partial t} - u\left(\frac{\partial \rho}{\partial t} + \nabla \cdot \left(\rho \vec{V}\right)\right) + \nabla \cdot \left(\rho u \vec{V}\right) \tag{3.20}$$

The term in bracket in 3.19 is identical to the left-hand side of the continuity equation in 3.7, hence, zero. Thus, 3.20 reduce to;

$$\rho \frac{Du}{Dt} = \frac{\partial(\rho u)}{\partial t} + \nabla \cdot \left(\rho u \vec{V}\right)$$

Substituting into 3.14 results in;

$$\frac{\partial(\rho u)}{\partial t} + \nabla \cdot \left(\rho u \vec{V}\right) = \left(-\frac{\partial P}{\partial x} + \frac{\partial \tau_{xx}}{\partial x} + \frac{\partial \tau_{yx}}{\partial y} + \frac{\partial \tau_{zx}}{\partial z}\right) + \rho f_x \tag{3.21}$$

Equation 3.22 is the conservation component of the momentum equation in the x - direction.

Similarly, in the y and z directions the momentum equations are respectively;

$$\frac{\partial(\rho v)}{\partial t}+\nabla\cdot\left(\rho v\vec{V}\right)=\left(-\frac{\partial P}{\partial y}+\frac{\partial \tau_{xy}}{\partial x}+\frac{\partial \tau_{yy}}{\partial y}+\frac{\partial \tau_{zy}}{\partial z}\right)+\rho f_y$$

$$\frac{\partial(\rho w)}{\partial t}+\nabla\cdot\left(\rho w\vec{V}\right)=\left(-\frac{\partial P}{\partial z}+\frac{\partial \tau_{xz}}{\partial x}+\frac{\partial \tau_{yz}}{\partial y}+\frac{\partial \tau_{zz}}{\partial z}\right)+\rho f_z$$

Sir Isaac Newton observed that the shear stress in a fluid was proportional to the time-rate-of-strain (velocity gradient). Such fluids are called Newtonian fluids. For such type of fluids, Stokes in 1845 obtained the following shear stress relations;

$$\begin{aligned}&\tau_{xx}=\lambda\nabla\cdot\vec{V}+2\mu\frac{\partial u}{\partial x},\tau_{yy}=\lambda\nabla\cdot\vec{V}+2\mu\frac{\partial v}{\partial y},\tau_{zz}=\lambda\nabla\cdot\vec{V}+2\mu\frac{\partial w}{\partial z},\\&\tau_{xy}=\tau_{yx}=\mu\left(\frac{\partial v}{\partial x}+\frac{\partial u}{\partial y}\right),\tau_{xz}=\tau_{zx}=\mu\left(\frac{\partial u}{\partial z}+\frac{\partial w}{\partial x}\right),\tau_{yz}=\tau_{zy}=\mu\left(\frac{\partial w}{\partial y}+\frac{\partial v}{\partial z}\right),\end{aligned} \qquad (3.22)$$

where μ is the molecular viscosity coefficient and λ is the bulk viscosity coefficient.

Stokes also hypothesised that; $\lambda=-\frac{2}{3}\mu$

Substituting respective terms of 3.22 into 3.21 produces the complete conservation form of the Navier - Stoke equations in the x direction as;

$$\frac{\partial(\rho u)}{\partial t}+\frac{\partial(\rho u^2)}{\partial x}+\frac{\partial(\rho uv)}{\partial y}+\frac{\partial(\rho uw)}{\partial z}=-\frac{\partial P}{\partial x}+\frac{\partial}{\partial x}\left(\lambda\nabla\cdot\vec{V}+2\mu\frac{\partial u}{\partial x}\right)+$$
$$\frac{\partial}{\partial y}\left(\mu\left(\frac{\partial v}{\partial x}+\frac{\partial u}{\partial y}\right)\right)+\frac{\partial}{\partial z}\left(\mu\left(\frac{\partial u}{\partial z}+\frac{\partial w}{\partial x}\right)\right)+\rho f_x$$

Similarly, in the y and z directions;

$$\frac{\partial(\rho v)}{\partial t}+\frac{\partial(\rho uv)}{\partial x}+\frac{\partial(\rho v^2)}{\partial y}+\frac{\partial(\rho vw)}{\partial z}=-\frac{\partial P}{\partial y}+\frac{\partial}{\partial x}\left(\mu\left(\frac{\partial v}{\partial x}+\frac{\partial u}{\partial y}\right)\right)+$$

$$\frac{\partial}{\partial y}\left(\lambda\nabla\cdot\vec{V}+2\mu\frac{\partial v}{\partial y}\right)+\frac{\partial}{\partial z}\left(\mu\left(\frac{\partial w}{\partial y}+\frac{\partial v}{\partial z}\right)\right)+\rho f_y$$

and

$$\frac{\partial(\rho w)}{\partial t}+\frac{\partial(\rho uw)}{\partial x}+\frac{\partial(\rho vw)}{\partial y}+\frac{\partial(\rho w^2)}{\partial z}=-\frac{\partial P}{\partial z}+\frac{\partial}{\partial x}\left(\mu\left(\frac{\partial u}{\partial z}+\frac{\partial w}{\partial x}\right)\right)+$$

$$\frac{\partial}{\partial y}\left(\mu\left(\frac{\partial w}{\partial y}+\frac{\partial v}{\partial z}\right)\right)+\frac{\partial}{\partial z}\left(\lambda\nabla\cdot\vec{V}+2\mu\frac{\partial w}{\partial z}\right)+\rho f_z$$

In vector form, we have;

$$\rho\frac{DU}{Dt}=-\nabla P+\left(\frac{1}{3}\mu+\lambda\right)\nabla(\nabla\cdot U)+\mu\nabla^2U+\rho f_B \qquad (3.23)$$

where the last term on the right represent the body force term of the momentum equation.

3.4 The Principles of Energy Conservation

According to the first law of thermodynamics the energy of a body is conserved. Hence the energy of the fluid in the control volume must be conserved. This implies that,

$$\begin{Bmatrix}\text{Rate of change of}\\ \text{energy inside the}\\ \text{fluid element}\end{Bmatrix}=\begin{Bmatrix}\text{Net flux of heat}\\ \text{into}\\ \text{the fluid element}\end{Bmatrix}+\begin{Bmatrix}\text{Rate of work done}\\ \text{due to body and}\\ \text{surface forces}\end{Bmatrix}$$

or $\quad A \quad = \quad B \quad + \quad C \qquad (3.24)$

where A, B and C denote the respective terms above.

The rate of work done by the body force acting on the fluid element moving at a velocity V is $\rho\vec{f}\cdot\vec{V}dxdydz$

For the surface forces, the pressure plus shear and normal stresses, we consider the forces in the $x-$ direction as shown in the Figure 3.4;

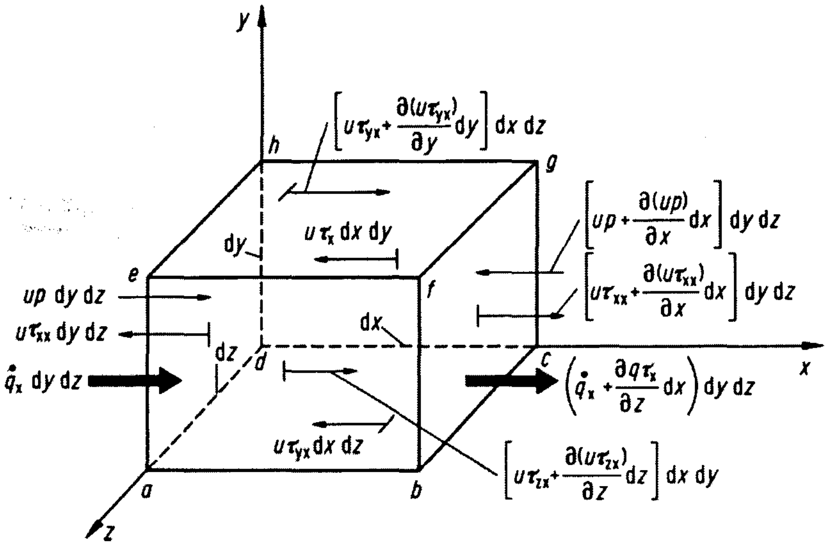

Figure 3.4: Energy fluxes associated with an infinitesimally small fluid element.

The rate of work done on the moving fluid element by the pressure and shear forces in the $x-$ direction is obtained by multiplying the $x-$ component of the velocity, u by the forces. Hence, work done on face $abcd$ by $\tau_{yx}dxdz$ is $u\tau_{yx}dxdz$ as shown in Figure 3.4. Similarly, works done on the other planes of $x-$ direction are indicated as above. Therefore, the net rate of work done by pressure in the $x-$ direction is

$$\left[up-\left(up+\frac{\partial(up)}{\partial x}dx\right)\right]dydz=-\frac{\partial(up)}{\partial x}dxdydz$$

Also, the net rate of work done by the shear stresses in the $x-$ direction on the $y-$ plane, that is on face $abcd$ and $efgh$ is

$$\left[\left(u\tau_{yx} + \frac{\partial(u\tau_{yx})}{\partial y}dy\right) - u\tau_{yx}\right]dxdz = \frac{\partial(u\tau_{yx})}{\partial y}dxdydz$$

Similarly, the net rate of work done by shear stresses in the $x-$ direction on the x planes (i.e. face $adeh$ and $bcfg$) is

$$\left[\left(u\tau_{xx} + \frac{\partial(u\tau_{xx})}{\partial x}dx\right) - u\tau_{xx}\right]dydz = \frac{\partial(u\tau_{xx})}{\partial x}dxdydz$$

The net rate of work done by shear stresses in the $x-$ direction on the $z - plane$ (i.e. face $abef$ and $cdhg$ is;

$$\left[\left(u\tau_{zx} + \frac{\partial(u\tau_{zx})}{\partial z}dz\right) - u\tau_{zx}\right]dxdy = \frac{\partial(u\tau_{zx})}{\partial z}dxdydz$$

Hence the net pressure and surface forces in the $x-$ direction is

$$\left[-\frac{\partial(up)}{\partial x} + \frac{\partial(u\tau_{xx})}{\partial x} + \frac{\partial(u\tau_{yx})}{\partial y} + \frac{\partial(u\tau_{zx})}{\partial z}\right]dxdydz$$

In the above expression, only surface forces in the $x-$ direction are considered. When surface forces in the y and z directions are included, the net pressure and surface forces would be respectively,

$$\left[-\frac{\partial(vp)}{\partial y} + \frac{\partial(v\tau_{xy})}{\partial x} + \frac{\partial(v\tau_{yy})}{\partial y} + \frac{\partial(v\tau_{zy})}{\partial z}\right]dxdydz$$

and

$$\left[-\frac{\partial(wp)}{\partial z}+\frac{\partial(w\tau_{xz})}{\partial x}+\frac{\partial(w\tau_{yz})}{\partial y}+\frac{\partial(w\tau_{zz})}{\partial z}\right]dxdydz$$

The net rate of work done on the moving fluid element is the sum of the surface force contributions in the x, y and $z-$ directions as well as the body force, hence C in equation 3.24 will be;

$$C=-\left(\frac{\partial(up)}{\partial x}+\frac{\partial(vp)}{\partial y}+\frac{\partial(wp)}{\partial z}\right)dxdydz+\left(\frac{\partial(u\tau_{xx})}{\partial x}+\frac{\partial(u\tau_{yx})}{\partial y}+\frac{\partial(u\tau_{zx})}{\partial z}\right)dxdydz+$$
$$\left(\frac{\partial(v\tau_{xy})}{\partial x}+\frac{\partial(v\tau_{yy})}{\partial y}+\frac{\partial(v\tau_{zy})}{\partial z}\right)dxdydz+\left(\frac{\partial(w\tau_{xz})}{\partial x}+\frac{\partial(w\tau_{yz})}{\partial y}+\frac{\partial(w\tau_{zz})}{\partial z}\right)dxdydz+ \quad (3.25)$$
$$\rho\vec{f}\cdot\vec{V}dxdydz$$

The net heat flux into the control volume is due to volumetric heating such as absorption or emission of radiation across the surface due to temperature gradients as a result of thermal conduction. We define $\dot{q}$ as the rate of volumetric heat addition per unit mass.

Since the mass of the moving fluid element is $\rho dxdydz$ then,

$$\begin{Bmatrix}Volumetric\ heating\\ of\ the\ element\end{Bmatrix}=\rho\dot{q}dxdydz$$

Heat transferred by thermal conduction into the moving fluid element across face *adhe* is

$$\left[\dot{q}_x+\left(\frac{\partial\dot{q}_x}{\partial x}\right)dx\right]dydz$$

Therefore the net heat transferred in the $x-$ direction into the fluid element by thermal conduction is

$$\left[\dot{q}_x - \left(\dot{q}_x + \frac{\partial \dot{q}_x}{\partial x}\right)dx\right]dydz = -\frac{\partial \dot{q}_x}{\partial x}dxdydz \tag{3.26a}$$

Similarly, the net heat transferred in the y and $z-$ directions are respectively,

$$\left[\dot{q}_y - \left(\dot{q}_y + \frac{\partial \dot{q}_y}{\partial y}\right)dy\right]dxdz = -\frac{\partial \dot{q}_y}{\partial y}dxdydz \tag{3.26b}$$

$$\left[\dot{q}_z - \left(\dot{q}_z + \frac{\partial \dot{q}_z}{\partial z}\right)dy\right]dxdz = -\frac{\partial \dot{q}_z}{\partial z}dxdydz \tag{3.26c}$$

Summing the resulting terms in equations 3.26a, 3.26b and 3.26c results in;

$$\begin{Bmatrix} \text{Heating of the fluid element} \\ \text{by thermal conduction} \end{Bmatrix} = -\left(\frac{\partial \dot{q}_x}{\partial x} + \frac{\partial \dot{q}_y}{\partial y} + \frac{\partial \dot{q}_z}{\partial z}\right)dxdydz$$

The net heat flux in the fluid element in equation 3.24 is;

$$B = \left[\rho\dot{q} - \left(\frac{\partial \dot{q}_x}{\partial x} + \frac{\partial \dot{q}_y}{\partial y} + \frac{\partial \dot{q}_z}{\partial z}\right)\right]dxdydz \tag{3.27}$$

Heat transfer by thermal conduction is proportional to the local temperature gradient hence:

$$\dot{q}_x = -k\frac{\partial T}{\partial x}, \quad \dot{q}_y = -k\frac{\partial T}{\partial y}, \quad \text{and} \quad \dot{q}_z = -k\frac{\partial T}{\partial z}, \tag{3.28}$$

where k is the thermal conductivity. Substituting respective terms of equation 3.28 into 3.27, we have;

$$B = \left[\rho\dot{q} + \frac{\partial}{\partial x}\left(k\frac{\partial T}{\partial x}\right) + \frac{\partial}{\partial y}\left(k\frac{\partial T}{\partial y}\right) + \frac{\partial}{\partial z}\left(k\frac{\partial T}{\partial z}\right) \right] dxdydz \tag{3.29}$$

The total energy of a moving fluid per unit mass is the sum of its internal energy per unit mass, e, and its kinetic energy per unit mass, $V^2/2$. Hence, the total energy per unit mass is $\left(e + \frac{V^2}{2}\right)$. Since a moving fluid element is followed, the time-rate-of-change of energy per unit mass is given by the substantial derivative. The mass of the fluid element is $\rho dxdydz$, hence we obtain 'A' in equation 3.24 as;

$$A = \rho\frac{D}{Dt}\left(e + \frac{V^2}{2}\right) dxdydz \tag{3.30}$$

The final form of the energy equation is obtained by substituting equation 3.25, 3.29, and 3.30 into equation 3.24 to get:

$$\begin{aligned} \rho\frac{D}{Dt}\left(e + \frac{V^2}{2}\right) = {} & \rho\dot{q} + \frac{\partial}{\partial x}\left(k\frac{\partial T}{\partial x}\right) + \frac{\partial}{\partial y}\left(k\frac{\partial T}{\partial y}\right) + \frac{\partial}{\partial z}\left(k\frac{\partial T}{\partial z}\right) - \frac{\partial(up)}{\partial x} - \\ & \frac{\partial(vp)}{\partial y} - \frac{\partial(wp)}{\partial z} + \frac{\partial(u\tau_{xx})}{\partial x} + \frac{\partial(u\tau_{yx})}{\partial y} + \frac{\partial(u\tau_{zx})}{\partial z} + \frac{\partial(v\tau_{xy})}{\partial x} + \frac{\partial(v\tau_{yy})}{\partial y} + \\ & \frac{\partial(v\tau_{zy})}{\partial z} + \frac{\partial(w\tau_{xz})}{\partial x} + \frac{\partial(w\tau_{yz})}{\partial y} + \frac{\partial(w\tau_{zz})}{\partial z} + \rho\vec{f}\cdot\vec{V} \end{aligned} \tag{3.31}$$

The momentum of the fluid element in the x, y and z directions are obtained respectively as;

$$\rho\frac{Du}{Dt} = -\frac{\partial P}{\partial x} + \frac{\partial \tau_{xx}}{\partial x} + \frac{\partial \tau_{yx}}{\partial y} + \frac{\partial \tau_{zx}}{\partial z} + \rho f_x$$

$$\rho\frac{Dv}{Dt} = -\frac{\partial P}{\partial y} + \frac{\partial \tau_{xy}}{\partial x} + \frac{\partial \tau_{yy}}{\partial y} + \frac{\partial \tau_{zy}}{\partial z} + \rho f_y \qquad (3.32)$$

$$\rho\frac{Dw}{Dt} = -\frac{\partial P}{\partial z} + \frac{\partial \tau_{xz}}{\partial x} + \frac{\partial \tau_{yz}}{\partial y} + \frac{\partial \tau_{zz}}{\partial z} + \rho f_z$$

Integrating each of the equations in 3.32 with respect to u, v and w respectively yields:

$$\rho\frac{Du^2/2}{Dt} = -\frac{\partial uP}{\partial x} + \frac{\partial u\tau_{xx}}{\partial x} + \frac{\partial u\tau_{yx}}{\partial y} + \frac{\partial u\tau_{zx}}{\partial z} + \rho u f_x$$

$$\rho\frac{Dv^2/2}{Dt} = -\frac{\partial vP}{\partial y} + \frac{\partial v\tau_{xy}}{\partial x} + \frac{\partial v\tau_{yy}}{\partial y} + \frac{\partial v\tau_{zy}}{\partial z} + \rho v f_y \qquad (3.33)$$

$$\rho\frac{Dw^2/2}{Dt} = -\frac{\partial wP}{\partial z} + \frac{\partial w\tau_{xz}}{\partial x} + \frac{\partial w\tau_{yz}}{\partial y} + \frac{\partial w\tau_{zz}}{\partial z} + \rho w f_z$$

Adding the equations in 3.33 and noting that $u^2 + v^2 + w^2 = V^2$ we obtained;

$$\rho\frac{DV^2/2}{Dt} = -u\frac{\partial P}{\partial x} - v\frac{\partial P}{\partial y} - w\frac{\partial P}{\partial x} + u\left(\frac{\partial \tau_{xx}}{\partial x} + \frac{\partial \tau_{yx}}{\partial y} + \frac{\partial \tau_{zx}}{\partial z}\right) +$$

$$v\left(\frac{\partial \tau_{xy}}{\partial x} + \frac{\partial \tau_{yy}}{\partial y} + \frac{\partial v\tau_{zy}}{\partial z}\right) + w\left(\frac{\partial \tau_{xz}}{\partial x} + \frac{\partial \tau_{yz}}{\partial y} + \frac{\partial v\tau_{zz}}{\partial z}\right) + \rho\left(uf_x + vf_y + wf_z\right) \qquad (3.34)$$

Subtracting equation 3.34 from 3.31 and noting that $\rho\vec{f}\cdot\vec{V} = \rho\left(uf_x + vf_y + wf_z\right)$ yield;

$$\rho\frac{De}{Dt} = \rho\dot{q} + \frac{\partial}{\partial x}\left(k\frac{\partial T}{\partial x}\right) + \frac{\partial}{\partial y}\left(k\frac{\partial T}{\partial y}\right) + \frac{\partial}{\partial z}\left(k\frac{\partial T}{\partial z}\right) - p\left(\frac{\partial u}{\partial x} + \frac{\partial v}{\partial y} + \frac{\partial w}{\partial z}\right)$$

$$+\tau_{xx}\frac{\partial u}{\partial x} + \tau_{yx}\frac{\partial u}{\partial y} + \tau_{zx}\frac{\partial u}{\partial z} + \tau_{xy}\frac{\partial v}{\partial x} + \tau_{yy}\frac{\partial v}{\partial y} + \tau_{zy}\frac{\partial v}{\partial z} \qquad (3.35)$$

$$+\tau_{xz}\frac{\partial w}{\partial x} + \tau_{yz}\frac{\partial w}{\partial y} + \tau_{zz}\frac{\partial w}{\partial z}$$

Equation 3.35 is the energy equation in terms of internal energy (e). This is the non-conservative form of the energy equation. Substituting respective terms in equation 3.22 into 3.35 yields the energy equation in terms of the flow-field variables as follows:

$$\rho\frac{De}{Dt}=\rho\dot{q}+\frac{\partial}{\partial x}\left(k\frac{\partial T}{\partial x}\right)+\frac{\partial}{\partial y}\left(k\frac{\partial T}{\partial y}\right)+\frac{\partial}{\partial z}\left(k\frac{\partial T}{\partial z}\right)-$$
$$p\left(\frac{\partial u}{\partial x}+\frac{\partial v}{\partial y}+\frac{\partial w}{\partial z}\right)+\lambda\left(\frac{\partial u}{\partial x}+\frac{\partial v}{\partial y}+\frac{\partial w}{\partial z}\right)^2+ \tag{3.36}$$
$$\mu\left(2\left(\frac{\partial u}{\partial x}\right)^2+2\left(\frac{\partial v}{\partial y}\right)^2+2\left(\frac{\partial w}{\partial z}\right)^2+\left(\frac{\partial u}{\partial y}+\frac{\partial v}{\partial x}\right)^2+\left(\frac{\partial u}{\partial z}+\frac{\partial w}{\partial x}\right)^2+\left(\frac{\partial v}{\partial z}+\frac{\partial w}{\partial y}\right)^2\right)$$

The energy equation in the conservation form can be obtained by considering the term in the left hand side of equation 3.36. The definition of substantial derivative implies that:

$$\rho\frac{De}{Dt}=\rho\frac{\partial e}{\partial t}+\rho\vec{V}.\nabla e \tag{3.37}$$

However,

$$\frac{\partial(\rho e)}{\partial t}=\rho\frac{\partial e}{\partial t}+e\frac{\partial \rho}{\partial t}$$
$$or \tag{3.38}$$
$$\rho\frac{\partial e}{\partial t}=\frac{\partial(\rho e)}{\partial t}-e\frac{\partial \rho}{\partial t}$$

From the vector identity concerning the divergence of the product of a scalar and a vector,

$$\nabla \cdot (\rho e \vec{V}) = e\nabla \cdot (\rho \vec{V}) + \rho \vec{V} \cdot \nabla e$$

$$or \qquad (3.39)$$

$$\rho \vec{V} \cdot \nabla e = \nabla \cdot (\rho e \vec{V}) - e\nabla \cdot (\rho \vec{V})$$

Substituting 3.38 and 3.39 into equation 3.37 results in;

$$\rho \frac{De}{Dt} = \frac{\partial(\rho e)}{\partial t} - e\left[\frac{\partial \rho}{\partial t} + \nabla \cdot (\rho \vec{V})\right] + \nabla \cdot (\rho e \vec{V}) \qquad (3.40)$$

The term in squared brackets in equation 3.40 is zero, from the continuity equation, hence equation 3.40 becomes;

$$\rho \frac{De}{Dt} = \frac{\partial(\rho e)}{\partial t} + \nabla \cdot (\rho e \vec{V}) \qquad (3.41)$$

Substituting 3.40 into 3.36 yields;

$$\frac{\partial(\rho e)}{\partial t} + \nabla \cdot (\rho e \vec{V}) = \rho \dot{q} + \frac{\partial}{\partial x}\left(k\frac{\partial T}{\partial x}\right) + \frac{\partial}{\partial y}\left(k\frac{\partial T}{\partial y}\right) + \frac{\partial}{\partial z}\left(k\frac{\partial T}{\partial z}\right) -$$

$$p\left(\frac{\partial u}{\partial x} + \frac{\partial v}{\partial y} + \frac{\partial w}{\partial z}\right) + \left(\frac{\partial u}{\partial x} + \frac{\partial v}{\partial y} + \frac{\partial w}{\partial z}\right)^2 + \qquad (3.42)$$

$$\mu\left(2\left(\frac{\partial u}{\partial x}\right)^2 + 2\left(\frac{\partial v}{\partial y}\right)^2 + 2\left(\frac{\partial w}{\partial z}\right)^2 + \left(\frac{\partial u}{\partial y} + \frac{\partial v}{\partial x}\right)^2 + \left(\frac{\partial u}{\partial z} + \frac{\partial w}{\partial x}\right)^2 + \left(\frac{\partial v}{\partial z} + \frac{\partial w}{\partial y}\right)^2\right)$$

Equation 3.42 is the conservation form of the energy equation, written in terms of internal energy.

In terms of total energy, equation 3.41 can be written as;

$$\rho\frac{D\left(e+\frac{V^2}{2}\right)}{Dt}=\frac{\partial}{\partial t}\left[\rho\left(e+\frac{V^2}{2}\right)\right]+\nabla\cdot\left[\rho\left(e+\frac{V^2}{2}\right)\vec{V}\right] \tag{3.43}$$

Substituting 3.43 into the left hand side of equation 3.31 yields;

$$\begin{aligned}&\frac{\partial}{\partial t}\left[\rho\left(e+\frac{V^2}{2}\right)\right]+\nabla\cdot\left[\rho\left(e+\frac{V^2}{2}\right)\vec{V}\right]=\rho\dot{q}+\frac{\partial}{\partial x}\left(k\frac{\partial T}{\partial x}\right)+\frac{\partial}{\partial y}\left(k\frac{\partial T}{\partial y}\right)+\\&\frac{\partial}{\partial z}\left(k\frac{\partial T}{\partial z}\right)-\frac{\partial(up)}{\partial x}-\frac{\partial(vp)}{\partial y}-\frac{\partial(wp)}{\partial z}+\frac{\partial(u\tau_{xx})}{\partial x}+\frac{\partial(u\tau_{yx})}{\partial y}+\frac{\partial(u\tau_{zx})}{\partial z}+\\&\frac{\partial(v\tau_{xy})}{\partial x}+\frac{\partial(v\tau_{yy})}{\partial y}+\frac{\partial(v\tau_{zy})}{\partial z}+\frac{\partial(w\tau_{xz})}{\partial x}+\frac{\partial(w\tau_{yz})}{\partial y}+\frac{\partial(w\tau_{zz})}{\partial z}+\rho\vec{f}\cdot\vec{V}\end{aligned} \tag{3.44}$$

Equation 3.44 is the conservation form of the energy equation written in terms of total energy.

Substituting respective terms of equation 3.22 into equation 3.44 we obtained;

$$\begin{aligned}&\frac{\partial}{\partial t}\left[\rho\left(e+\frac{V^2}{2}\right)\right]+\nabla\cdot\left[\rho\left(e+\frac{V^2}{2}\right)\vec{V}\right]=\rho\dot{q}+\frac{\partial}{\partial x}\left(k\frac{\partial T}{\partial x}\right)+\frac{\partial}{\partial y}\left(k\frac{\partial T}{\partial y}\right)+\\&\frac{\partial}{\partial z}\left(k\frac{\partial T}{\partial z}\right)-\frac{\partial(up)}{\partial x}-\frac{\partial(vp)}{\partial y}-\frac{\partial(wp)}{\partial z}+\lambda\left(\frac{\partial u}{\partial x}+\frac{\partial v}{\partial y}+\frac{\partial w}{\partial z}\right)^2+\\&\mu\left(2\left(\frac{\partial u}{\partial x}\right)^2+2\left(\frac{\partial v}{\partial y}\right)^2+2\left(\frac{\partial w}{\partial z}\right)^2+\left(\frac{\partial u}{\partial y}+\frac{\partial v}{\partial x}\right)^2+\left(\frac{\partial u}{\partial z}+\frac{\partial w}{\partial x}\right)^2+\left(\frac{\partial v}{\partial z}+\frac{\partial w}{\partial y}\right)^2\right)+\\&\rho\vec{f}\cdot\vec{V}\end{aligned}$$

This simplifies to;

$$\frac{\partial}{\partial t}\left[\rho\left(e+\frac{V^2}{2}\right)\right]+\nabla\cdot\left[\rho\left(e+\frac{V^2}{2}\right)\vec{V}\right]=\rho\dot{q}+\frac{\partial}{\partial x}\left(k\frac{\partial T}{\partial x}\right)+\frac{\partial}{\partial y}\left(k\frac{\partial T}{\partial y}\right)+$$
$$\frac{\partial}{\partial z}\left(k\frac{\partial T}{\partial z}\right)-\frac{\partial(up)}{\partial x}-\frac{\partial(vp)}{\partial y}-\frac{\partial(wp)}{\partial z}+\mu\Phi+\rho\vec{f}\cdot\vec{V} \tag{3.45}$$

Where,

$$\Phi=\left(2\left(\frac{\partial u}{\partial x}\right)^2+2\left(\frac{\partial v}{\partial y}\right)^2+2\left(\frac{\partial w}{\partial z}\right)^2+\left(\frac{\partial u}{\partial y}+\frac{\partial v}{\partial x}\right)^2+\left(\frac{\partial u}{\partial z}+\frac{\partial w}{\partial x}\right)^2+\left(\frac{\partial v}{\partial z}+\frac{\partial w}{\partial y}\right)^2\right)+\lambda\left(\frac{\partial u}{\partial x}+\frac{\partial v}{\partial y}+\frac{\partial w}{\partial z}\right)^2$$

The internal energy of the incompressible flows, 3.45 simplifies to;

$$\rho\left[\frac{\partial e}{\partial t}+u\frac{\partial e}{\partial x}+v\frac{\partial e}{\partial y}+w\frac{\partial e}{\partial z}\right]=k\left(\frac{\partial^2 T}{\partial x^2}+\frac{\partial^2 T}{\partial y^2}+\frac{\partial^2 T}{\partial z^2}\right)+\mu\Phi$$

Where $\partial e=c_v\partial T$ and $c_v=c_p$ for incompressible flows, the generalized thermal energy equation is obtained as;

$$\rho C_p\left[\frac{\partial T}{\partial t}+u\frac{\partial T}{\partial x}+v\frac{\partial T}{\partial y}+w\frac{\partial T}{\partial z}\right]=k\left(\frac{\partial^2 T}{\partial x^2}+\frac{\partial^2 T}{\partial y^2}+\frac{\partial^2 T}{\partial z^2}\right)+\mu\Phi \tag{3.46}$$

3.5 Conservation of Chemical Species Concentration

If the viscous fluid consists of a binary mixture in which there are species concentration gradients (Figure 2.4), there will be relative transport of the species, and species conservation must be satisfied at each point in the fluid. The pertinent form of the conservation equation may be obtained by identifying the processes that affect the *transport* and *generation* of species A for a differential control volume in the fluid.

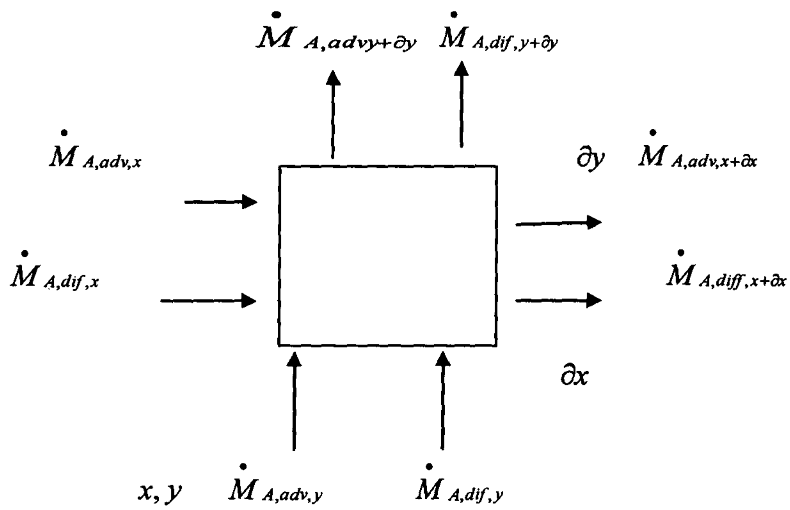

Figure 3.5 Species conservation in two-dimensional flow of a viscous fluid

Consider the control volume of Figure 3.5 where Species A may be transported by *advection* (with the mean velocity of the mixture) and by *diffusion* (relative to the mean motion) in each of the coordinate directions. The concentration may also be affected by chemical reactions, and the rate at which the mass of species A is generated per unit volume due to such reactions is designated by $\dot{n}_A$. The *net* rate at which species A *enters* the control volume due to *advection* in the *x*-direction is;

$$\dot{M}_{A,adv,x}-\dot{M}_{A,advx+\partial x}=(\rho_A u)-\left[(\rho_A u)+\frac{\partial(\rho_A u)}{\partial x}\partial x\right]\partial y=\frac{\partial(\rho_A u)}{\partial x}\partial x\partial y \tag{3.47}$$

Similarly, multiplying both sides of the Fick's law by the molecular weight M_A (kg/mol) of species A to evaluate the diffusion flux, the *net* rate at which species A *enters* the control volume due to *diffusion* in the *x*-direction is:

$$\dot{M}_{A,dif,x} - \dot{M}_{A,dif,x+\partial x} = \left(-D_{AB}\frac{\partial \rho_A}{\partial x}\right)\partial y - \left[\left(-D_{AB}\frac{\partial \rho_A}{\partial x}\right) + \frac{\partial}{\partial x}\left(-D_{AB}\frac{\partial \rho_A}{\partial x}\partial x\right)\right]\partial y$$
$$= \frac{\partial}{\partial x}\left(D_{AB}\frac{\partial \rho_A}{\partial x}\right)\partial x \partial y \qquad (3.48)$$

Expressions similar to equations 3.47 and 3.48 may be formulated for the *y*-direction. Referring to Figure 3.5, the species conservation requirement is

$$\dot{M}_{A,adv,x} - \dot{M}_{A,advx+\partial x} + \dot{M}_{A,adv,y} - \dot{M}_{A,advy+\partial y} + \dot{M}_{A,dif,x} -$$
$$\dot{M}_{A,dif,x+\partial x} + \dot{M}_{A,dif,y} - \dot{M}_{A,dif,x+\partial y} - \dot{M}_{A,d} = 0 \qquad (3.49)$$

Substituting from equations 3.47 and 3.48, as well as from similar forms for the *y*-direction, it follows that,

$$\frac{\partial(\rho_A u)}{\partial x} + \frac{\partial(\rho_A v)}{\partial y} = \frac{\partial}{\partial x}\left(D_{AB}\frac{\partial \rho_A}{\partial x}\right) + \frac{\partial}{\partial y}\left(D_{AB}\frac{\partial \rho_A}{\partial y}\right) + \dot{n}_A \qquad (3.50)$$

A more useful form of this equation may be obtained by expanding the terms on the left-hand side of (3.50). Substituting from the overall continuity equation for an incompressible fluid reduces equation 3.50 to:

$$u\frac{\partial \rho_A}{\partial x} + v\frac{\partial \rho_A}{\partial y} = \frac{\partial}{\partial x}\left(D_{AB}\frac{\partial \rho_A}{\partial x}\right) + \frac{\partial}{\partial y}\left(D_{AB}\frac{\partial \rho_A}{\partial y}\right) + \dot{n}_A$$

or in Molar form to:

$$u\frac{\partial C_A}{\partial x} + v\frac{\partial C_A}{\partial y} = \frac{\partial}{\partial x}\left(D_{AB}\frac{\partial C_A}{\partial x}\right) + \frac{\partial}{\partial y}\left(D_{AB}\frac{\partial C_A}{\partial y}\right) + \dot{N}_A \qquad (3.51)$$

where C is the concentration, D is the molecular diffusivity and $\dot{N}_A$ is the rate at which the species A is generated/destructed per unit volume.

3.6 MHD Boundary Layer Flow past an Inclined Plate with Viscous Dissipation

The differential equations governing the flow of ferrofluid over inclined surfaces are modelled using the Navier – Stokes equations. The modelled equations are used to solve a problem commonly encountered in industry. Suitable similarity variables have been employed to reduce the partial differential equations to nonlinear higher order ordinary differential equations. The resulting equations are solved numerically and results presented graphically. A parametric analysis is conducted to examine the influence of various parameters on the velocity, temperature and concentration of the ferrofluid in the boundary layer. The plate was inclined at 6^o for the study, however to analyse the effect of inclination, angle used were 0^o, 6^o , 10^o, 15^o, 30^o, 60^o and 90^o. Other important parameters of interest such as the skin-friction coefficient, Nusselt number and the Sherwood numbers have been investigated. The values of a specific parameter of interest was increased whilst others were kept constant to study the effect of the parameter on the skin friction coefficient, rate of heat transfer, temperature of plate and rate of mass transfer.

3.6.1 The Mathematical Model Generation

An incompressible ferrofluid such as polyethylene oxide solution is assumed to flow uniformly over a heated plate with applied transverse magnetic field. A Cartesian coordinate system is adopted with the origin fixed in such a way that the $x-$axis is taken along the direction of the flat surface and the $y-$axis measured normal to the surface of the plate. A uniform heat is applied in the direction of the $y-$axis under the plate. The flow is induced by the combined effect of convection in the boundary layer and the angle of inclination. It is assumed that the fluid flows continuously over the flat plate with a uniform thickness h. In addition, the effect of viscous dissipation and chemical reaction are incorporated. The plate is then tilted to variable angles $\propto_i$, $i = 1,2,3,...7$ to study the effect of inclination of the flow on the flat plate (Fig. 3.6).

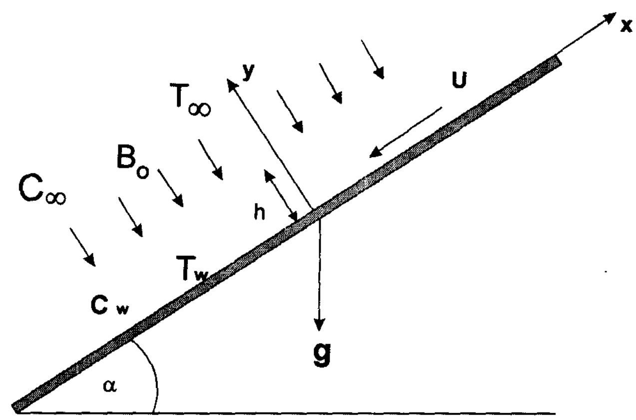

Fig. 3.6: Ferrofluid flowing over an Inclined Plate

The differential equations governing the flow are the continuity, momentum, energy and concentration equations along with appropriate boundary conditions.

3.6.2 Modeling the Continuity Equation

For two dimensional incompressible steady flows, equation 3.8 simplifies to;

$$\frac{\partial u}{\partial x} + \frac{\partial v}{\partial y} = 0 \tag{3.52}$$

3.6.3 Modelling the Momentum Equation for the problem

For incompressible viscous flow, the term $\nabla . U$ vanishes, thus equation 3.24 reduces to;

$$\rho \frac{DU}{Dt} = -\nabla P + \mu \nabla^2 U + \rho f_B$$

$$or \qquad (3.53)$$

$$\rho \frac{DU}{Dt} = \rho f_B - \nabla P + \mu \nabla^2 U$$

In this case, the body force ρf_B is that due to gravity, hence we have 3.53 transformed into:

$$\rho\left(\frac{\partial U}{\partial t} + \frac{\partial U}{\partial x} + \frac{\partial U}{\partial y} + \frac{\partial U}{\partial z}\right) = -\rho g - \left(\frac{\partial P}{\partial x} + \frac{\partial P}{\partial y} + \frac{\partial P}{\partial z}\right) +$$

$$\mu\left(\frac{\partial^2 U}{\partial x^2} + \frac{\partial^2 U}{\partial y^2} + \frac{\partial^2 U}{\partial z^2}\right)$$

For two dimensional incompressible steady flows we have;

$$\rho\left(\frac{\partial U}{\partial x} + \frac{\partial U}{\partial y}\right) = -\rho g - \left(\frac{\partial P}{\partial x} + \frac{\partial P}{\partial y}\right) + \mu\left(\frac{\partial^2 U}{\partial x^2} + \frac{\partial^2 U}{\partial y^2}\right) \qquad (3.54)$$

Since the fluid is flowing along the direction of the x axis, $\frac{\partial P}{\partial y} << \frac{\partial P}{\partial x}$ and $\frac{\partial^2 u}{\partial x^2} << \frac{\partial^2 u}{\partial y^2}$

hence equation 3.54 becomes; $\rho\left(\frac{\partial U}{\partial x} + \frac{\partial U}{\partial y}\right) = -\rho g - \frac{\partial P}{\partial x} + \mu \frac{\partial^2 U}{\partial y^2}$

Since the density of the mixture is a function of its temperature and mass fraction of its species, it can be expanded using a Taylor's series near the vicinity of a reference point (T_∞, C_∞) of a single chemically reacting element given by:

$$\rho = \rho_\infty + \frac{\partial \rho}{\partial T}(T - T_\infty) + \frac{\partial \rho}{\partial C}(C - C_\infty)$$

where ρ_∞ is the density at the reference point. By definition, the coefficient of thermal expansion β and composition coefficient of volume expansion β^* are respectively:

$$\beta_T = -\frac{1}{\rho_\infty}\left(\frac{\partial \rho}{\partial T}\right)_p \qquad \text{and} \qquad \beta_C = -\frac{1}{\rho_\infty}\left(\frac{\partial \rho}{\partial C}\right)_p$$

and neglecting the higher order terms in the Taylor's series expansion yields:

$$\rho = \rho_\infty - \rho_\infty \beta_T (T - T_\infty) - \rho_\infty \beta_C (C - C_\infty) \tag{3.55}$$

which is valid only if $\beta_T (T - T_\infty)$ and $\beta_C (C - C_\infty) << 1$

Substituting equation 3.55 into the momentum equation results in;

$$\rho\left(u\frac{\partial u}{\partial x} + v\frac{\partial u}{\partial y}\right) = -\rho_\infty g + \rho_\infty g\beta_T (T - T_\infty) + \rho_\infty g\beta_C (C - C_\infty) - \frac{\partial p}{\partial x} + \mu\left(\frac{\partial^2 u}{\partial x^2} + \frac{\partial^2 u}{\partial y^2}\right) \tag{3.56}$$

Dividing equation 3.57 by ρ reduces to:

$$u\frac{\partial u}{\partial x} + v\frac{\partial u}{\partial y} = -\frac{\rho_\infty}{\rho} g + g\beta_T (T - T_\infty) + g\beta_C (C - C_\infty) - \frac{1}{\rho}\frac{\partial p}{\partial x} + \frac{\mu}{\rho}\left(\frac{\partial^2 u}{\partial x^2} + \frac{\partial^2 u}{\partial y^2}\right) \tag{3.57}$$

Given that; $\frac{\partial p}{\partial x} = \frac{\partial p_\infty}{\partial x} = -\rho_\infty g$ (3.58)

Substituting equation 3.58 into 3.57 results in;

$$u\frac{\partial u}{\partial x} + v\frac{\partial u}{\partial y} = -\frac{\rho_\infty}{\rho} g + g\beta_T (T - T_\infty) + g\beta_C (C - C_\infty) + \frac{1}{\rho}.\rho_\infty g + \upsilon\left(\frac{\partial^2 u}{\partial x^2} + \frac{\partial^2 u}{\partial y^2}\right)$$

$$u\frac{\partial u}{\partial x}+v\frac{\partial u}{\partial y}=g\beta_T(T-T_\infty)+g\beta_C(C-C_\infty)+\upsilon\left(\frac{\partial^2 u}{\partial x^2}+\frac{\partial^2 u}{\partial y^2}\right)$$

Furthermore, in a boundary layer approximation, $\frac{\partial^2 u}{\partial x^2} << \frac{\partial^2 u}{\partial y^2}$,

Therefore the governing momentum equation becomes:

$$u\frac{\partial u}{\partial x}+v\frac{\partial u}{\partial y}=\upsilon\frac{\partial^2 u}{\partial y^2}+g\beta_T(T-T_\infty)+g\beta_C(C-C_\infty), \qquad (3.59)$$

where υ is the kinematic viscosity and g is gravitational acceleration.

For a porous inclined surface in the presence of transverse magnetic field, we modify the momentum equation to cater for the inclination Lorenz force components to obtain;

$$u\frac{\partial u}{\partial x}+v\frac{\partial u}{\partial y}=v\frac{\partial^2 u}{\partial y^2}+g\beta_T(T-T_\infty)\sin\alpha+g\beta_C(C-C_\infty)\sin\alpha-\frac{\sigma B_o^2}{\rho}u-\frac{v}{k}(u-U_\infty) \qquad (3.60)$$

3.6.4 Modelling the Energy Equation for the problem

The generalized form of the energy equation was derived in (3.46). For two dimensional flow;

$$\rho C_p\left[\frac{\partial T}{\partial t}+u\frac{\partial T}{\partial x}+v\frac{\partial T}{\partial y}\right]=k\left(\frac{\partial^2 T}{\partial x^2}+\frac{\partial^2 T}{\partial y^2}\right)+\mu\Phi$$

where $\Phi=2\left[\left(\frac{\partial u}{\partial x}\right)^2+\left(\frac{\partial v}{\partial y}\right)^2\right]+\left[\frac{\partial u}{\partial y}+\frac{\partial v}{\partial x}\right]^2-\frac{2}{3}\left[\frac{\partial u}{\partial x}+\frac{\partial v}{\partial y}\right]^2$ is the viscous dissipative term.

For a steady flow, $\frac{\partial T}{\partial t}=0$, hence, (3.60) reduces to:

$$\rho C_p\left[u\frac{\partial T}{\partial x}+v\frac{\partial T}{\partial y}\right]=k\left(\frac{\partial^2 T}{\partial x^2}+\frac{\partial^2 T}{\partial y^2}\right)+\mu\Phi \tag{3.61}$$

In boundary layer approximations, it is often observed that generally $\frac{\partial u}{\partial x} << \frac{\partial u}{\partial y}$, v << u

hence $\frac{\partial v}{\partial x}\approx\frac{\partial v}{\partial y}\approx 0$ and $\frac{\partial^2 T}{\partial x^2}<<\frac{\partial^2 T}{\partial y^2}$,

Hence the boundary layer form of the viscous dissipative term simplifies to: $\Phi=\left(\frac{\partial u}{\partial y}\right)^2$

Therefore $\rho C_p\left[u\frac{\partial T}{\partial x}+v\frac{\partial T}{\partial y}\right]=k\frac{\partial^2 T}{\partial y^2}+\mu\left(\frac{\partial u}{\partial y}\right)^2$

Or $u\frac{\partial T}{\partial x}+v\frac{\partial T}{\partial y}=\alpha\frac{\partial^2 T}{\partial y^2}+\frac{\upsilon}{c_p}\left(\frac{\partial u}{\partial y}\right)^2$, where $\alpha=\frac{k}{\rho c_p}$ and $\mu=\upsilon\rho$

The energy equation thus becomes:

$$u\frac{\partial T}{\partial x}+v\frac{\partial T}{\partial y}=\alpha\frac{\partial^2 T}{\partial y^2}+\frac{\upsilon}{c_p}\left(\frac{\partial u}{\partial y}\right)^2, \tag{3.62}$$

where υ is the kinematic viscosity, α is the thermal diffusivity and c_p is the specific heat at constant pressure. For steady two dimensional incompressible viscous flows over a heated porous plate in the presence of magnetic field, the energy equation is modified to incorporate the heat generation terms as;

$$u\frac{\partial T}{\partial x}+v\frac{\partial T}{\partial y}=\alpha_o\frac{\partial^2 T}{\partial y^2}+\frac{v}{c_p}\left(\frac{\partial u}{\partial y}\right)^2+\frac{v}{kc_p}u^2+\frac{\sigma B_o^2}{\rho c_p}u^2+\frac{Q_o}{\rho c_p}(T-T_\infty) \tag{3.63}$$

where B_0 is a constant magnetic field strength and Q_0 is the energy generation parameter.

3.6.5 Modelling the Concentration Equation for the Problem

The generalized concentration equation was derived from equation 3.51 as:

$$u\frac{\partial C_A}{\partial x}+v\frac{\partial C_A}{\partial y}=\frac{\partial}{\partial x}\left(D_{AB}\frac{\partial C_A}{\partial x}\right)+\frac{\partial}{\partial y}\left(D_{AB}\frac{\partial C_A}{\partial y}\right)+\dot{N}_A,$$

In boundary layer approximation, $\frac{\partial^2 C}{\partial x^2}<<\frac{\partial^2 C}{\partial y^2}$, so the equation reduces to:

$$u\frac{\partial C}{\partial x}+v\frac{\partial C}{\partial y}=D\frac{\partial^2 C}{\partial y^2}+\dot{N}_A \qquad (3.64)$$

Assuming that the chemical reaction leads to the destruction of species A, then the molar destruction rate can be defined as

$$\dot{N}_A=-\gamma C^n \quad \text{where } C=C-C_\infty, \qquad (3.65)$$

The index n represents the order of the reaction, γ is the plate surface rate of chemical reaction. Substituting (3.65) into (3.64) gives the concentration equation as;

$$u\frac{\partial C}{\partial x}+v\frac{\partial C}{\partial y}=D\frac{\partial^2 C}{\partial y^2}-\gamma(C-C_\infty)^n \qquad (3.66)$$

For first order chemical reaction $n = 1$, hence equation 3.64 becomes;

$$u\frac{\partial C}{\partial x}+v\frac{\partial C}{\partial y}=D\frac{\partial^2 C}{\partial y^2}-\gamma(C-C_\infty) \qquad (3.67)$$

3.6.6 The Boundary Conditions of the Model

The above governing equations generally require initial and boundary conditions to enable a solution. The boundary of the domain may either be solid or fluid and the computation domain comprises usually only a part of the whole flow field. For mass and momentum equations all velocity components are specified, for the energy and concentration equations, the values of the dependent variables such as the temperature and the concentration respectively at the wall and upstream are also specified. As the surface is a solid wall, no-slip condition is specified on the boundary.

The vertical and horizontal components of velocity at the wall are set to zero. The concentration at the wall is set to be C_w. It is also assumed that the plate is heated by convection from a hot fluid at temperature T_f which provides a heat transfer coefficient, h_f and the plate generates heat Q_o. Hence the wall surface velocity, temperature and concentration are;

$$u(x,0)=0,\ v(x,0)=0, -k\frac{\partial T}{\partial y}=h_f\left[T_f-T(x,0)\right] \text{ and } C(x,0)=C_w \tag{3.68}$$

The free stream velocity, temperature and concentration are as follows

$$u(x,\infty)\rightarrow U_\infty,\ T(x,\infty)\rightarrow T_\infty,\ C(x,\infty)\rightarrow C_\infty \tag{3.69}$$

3.7 The Numerical Procedure

Introducing the following non-dimensional variables, the partial differential equations are transformed to dimensionless equations;

$$\eta=y\left(\frac{U_\infty}{\nu x}\right)^{\frac{1}{2}}, \psi=\sqrt{\nu U_\infty x}\,f(\eta),\ \theta(\eta)=\frac{T-T_\infty}{T_w-T_\infty},\ \phi(\eta)=\frac{C-C_\infty}{C_w-C_\infty}, \tag{3.70}$$

where $\eta, \psi, \theta(\eta)$, and $\phi(\eta)$ are the dimensionless independent variable, stream function, temperature and concentration respectively.

The stream function and the velocity components relate in the usual way as;

$$u = \frac{\partial \psi}{\partial y} \text{ and } v = -\frac{\partial \psi}{\partial x}.$$

Using chain rule where; $u = \frac{\partial \psi}{\partial \eta} \cdot \frac{\partial \eta}{\partial y}$ and $v = -\frac{\partial \psi}{\partial \eta} \cdot \frac{\partial \eta}{\partial x}$

Thus, $\frac{\partial \psi}{\partial \eta} = \sqrt{(\upsilon x U_\infty)} f'(\eta)$ and $\frac{\partial \eta}{\partial y} = \sqrt{\left(\frac{U_\infty}{\upsilon x}\right)}$

Substituting, we obtained;

$$u = \frac{\partial \psi}{\partial y} = \sqrt{\nu U_\infty x} f'(\eta) \cdot \sqrt{\frac{U_\infty}{\nu x}} = U_\infty f'(\eta)$$

$$v = -\frac{\partial \psi}{\partial x} = -\left[\frac{1}{2}\sqrt{\frac{\nu U_\infty}{x}} f(\eta) - \frac{1}{2} y \sqrt{\left(\frac{\nu U_\infty}{x}\right)} \cdot \sqrt{\frac{U_\infty}{\nu x}} f'(\eta)\right] = \frac{1}{2}\sqrt{\frac{\nu U_\infty}{x}} [\eta f'(\eta) - f(\eta)]$$

as velocity components in the x and y directions.

3.7.1 Continuity of Flow

Differentiating u with respect to x leads to;

$$\frac{\partial u}{\partial x} = U_\infty f(\eta)\left(-\frac{1}{2}\right) \cdot y \cdot \left(\frac{U_\infty}{\nu}\right)^{\frac{1}{2}} x^{-\frac{3}{2}} = -\frac{1}{2}\frac{U_\infty}{x} \cdot \eta \cdot f''(\eta)$$

Also, differentiating v with respect to y leads to;

$$\frac{\partial v}{\partial y}=\frac{1}{2}\sqrt{\frac{\nu U_\infty}{x}}\left[\sqrt{\frac{U_\infty}{\nu x}}f'(\eta)+\eta\cdot f''(\eta)\cdot\sqrt{\left(\frac{U_\infty}{\nu x}\right)}-\sqrt{\frac{U_\infty}{\nu x}}f'(\eta)\right]=\frac{1}{2}\frac{U_\infty}{x}\cdot\eta\cdot f''(\eta)$$

Substituting $\frac{\partial u}{\partial x}$ and $\frac{\partial v}{\partial y}$ into the continuity equation satisfies it identically. Thus, the flow represents the case of a fluid which can be analyzed using the chosen similarity variables.

3.7.2 Dimensionless Momentum Equation

The terms in the momentum equation are transformed and then substituted into equation 3.60 as follows;

$$u\frac{\partial u}{\partial x}=U_\infty f'(\eta)\cdot\left[-\frac{1}{2}\frac{U_\infty}{x}\cdot\eta\cdot f''(\eta)\right]=-\frac{1}{2}\frac{U_\infty^2}{x}\cdot\eta\cdot f'(\eta)\cdot f''(\eta)\ ,\ \frac{\partial u}{\partial y}=U_\infty f''(\eta)\sqrt{\frac{U_\infty}{\nu x}}\ ,$$

and $$\frac{\partial^2 u}{\partial y^2}=\frac{U_\infty^2}{\nu x}f'''(\eta)$$

Also,

$$v\frac{\partial u}{\partial y}=\frac{1}{2}\sqrt{\frac{\nu U_\infty}{x}}[\eta\cdot f(\eta)-f(\eta)]\cdot U_\infty f''\cdot\sqrt{\frac{U_\infty}{\nu x}}=\frac{1}{2}\frac{U_\infty^2}{x}\cdot\eta\cdot f'(\eta)\cdot f''(\eta)-\frac{1}{2}\frac{U_\infty^2}{x}\cdot f(\eta)\cdot f''(\eta)$$

$$\nu\frac{\partial^2 u}{\partial y^2}=\nu\cdot\frac{U_\infty^2}{\nu x}\cdot f'''(\eta)=\frac{U_\infty^2}{x}\cdot f'''(\eta),\ \frac{\nu}{k}(u-U_\infty)=\frac{\nu}{k}(U_\infty f'(\eta)-U_\infty),$$

$$\frac{\sigma B_o^2}{\rho}u=\frac{\sigma B_o^2}{\rho}U_\infty f'(\eta)$$

Substituting the respective terms into the momentum equation 3.60 results in;

$$-\frac{1}{2}\frac{U_\infty^2}{x}\cdot\eta\cdot f'(\eta)\cdot f''(\eta)+\frac{1}{2}\frac{U_\infty^2}{x}\cdot\eta\cdot f'(\eta)\cdot f''(\eta)-\frac{1}{2}\frac{U_\infty^2}{x}\cdot f(\eta)\cdot f''(\eta)=$$
$$\frac{U_\infty^2}{\nu x}\cdot f'''(\eta)+g\beta_T(T-T_\infty)\sin\alpha+g\beta_C(C-C_\infty)\sin\alpha-\frac{\sigma B_o^2}{\rho}U_\infty f'(\eta)-\frac{\nu}{k}U_\infty f'(\eta)+\frac{\nu}{k}U_\infty$$

Simplifying and multiplying by $\frac{\nu x}{U_\infty^2}$ yields;

$$\cdot f'''(\eta)+\frac{1}{2}f'(\eta)\cdot f''(\eta)+g\beta\frac{x}{U_\infty^2}(T-T_\infty)\sin\alpha+g\beta^*\frac{x}{U_\infty^2}(C-C_\infty)\sin\alpha-$$
$$\frac{\sigma B_o^2}{\rho}\frac{x}{U_\infty}f'(\eta)-\frac{\nu}{k}\frac{x}{U_\infty}f'(\eta)+\frac{\nu}{k}\frac{x}{U_\infty}=0 \tag{3.71}$$

But, $Gr=\frac{g\beta_T x(T_w-T_\infty)}{U_\infty^2}, Gc=\frac{g\beta_C x(C_w-C_\infty)}{U_\infty^2}, \delta=\frac{\nu x}{\kappa U_\infty}, M=\frac{\sigma B_o^2 x}{\rho U_\infty}$

Substituting respective terms into equation 3.71 yields the transformed momentum equation as;

$$f'''+\frac{1}{2}f\cdot f''+Gr\cdot\theta\cdot\sin\alpha+Gc\cdot\phi\cdot\sin\alpha-(\delta+M)f'+\delta=0 \tag{3.72}$$

3.7.3 Dimensionless Energy Equation

The various terms of the energy equation are transformed into ordinary differential equations as follows;

$$T=T_\infty+\theta(\eta)(T_w-T_\infty)$$

Differentiating with respect to x using the chain rule yields;

$$\frac{\partial T}{\partial x}=-\frac{1}{2}(T_w-T_\infty)\cdot y\cdot\sqrt{\frac{U_\infty}{\nu}}\cdot x^{-3/2}\cdot\theta'(\eta)=-\frac{1}{2}(T_w-T_\infty)\cdot\frac{y}{x}\cdot\sqrt{\frac{U_\infty}{\nu x}}\cdot\theta'(\eta)$$

$$u\frac{\partial T}{\partial x} = U_\infty f'(\eta)\cdot\left[-\frac{1}{2}(T_w - T_\infty)\cdot\frac{y}{x}\cdot\sqrt{\frac{U_\infty}{\nu x}}\cdot\theta'(\eta)\right] = -\frac{1}{2}\frac{U_\infty}{x}(T_w - T_\infty)\cdot\eta\cdot f'(\eta)\cdot\theta'(\eta)$$

Also, differentiating T with respect to y results in;

$$\frac{\partial T}{\partial y} = (T_w - T_\infty)\cdot\sqrt{\frac{U_\infty}{\nu x}}\cdot\theta'(\eta),\ \frac{\partial^2 T}{\partial y^2} = (T_w - T_\infty)\cdot\sqrt{\frac{U_\infty}{\nu x}}\cdot\sqrt{\frac{U_\infty}{\nu x}}\cdot\theta''(\eta) = (T_w - T_\infty)\cdot\frac{U_\infty}{\nu x}\cdot\theta''(\eta)$$

Thus,

$$v\frac{\partial T}{\partial y} = \frac{1}{2}\sqrt{\frac{\nu U_\infty}{x}}[\eta\cdot f'(\eta) - f(\eta)]\cdot(T_w - T_\infty)\cdot\sqrt{\frac{U_\infty}{\nu x}}\cdot\theta'(\eta) = \frac{1}{2}\frac{U_\infty}{x}[\eta\cdot f'(\eta) - f(\eta)]\cdot(T_w - T_\infty)\cdot\theta'(\eta)$$

$$v\frac{\partial T}{\partial y} = \frac{1}{2}\frac{U_\infty}{x}\cdot\eta\cdot(T_w - T_\infty)f'(\eta)\cdot\theta'(\eta) - \frac{1}{2}\frac{U_\infty}{x}\cdot(T_w - T_\infty)\cdot f(\eta)\cdot\theta'(\eta)$$

$$\alpha\frac{\partial^2 T}{\partial y^2} = \alpha\cdot(T_w - T_\infty)\cdot\frac{U_\infty}{\nu x}\cdot\theta''(\eta) = \frac{U_\infty}{x}\cdot\frac{1}{\Pr}(T_w - T_\infty)\cdot\theta''(\eta)$$

where $\alpha = \nu/\Pr$

$$= Ec\cdot(T_w - T_\infty)\frac{U_\infty}{x}f''^2(\eta)$$

Since, $c_p = \dfrac{U_\infty^2}{Ec\cdot(T_w - T_\infty)}$

$$\frac{\nu}{k\cdot c_p}u^2 = \frac{\nu}{k\cdot c_p}\cdot(U_\infty f'(\eta))^2 = \frac{\nu}{k\cdot c_p}\cdot U_\infty^2 f'^2(\eta),\ c_p = \frac{x\nu U_\infty}{kN(T_w - T_\infty)}$$

$$\frac{\nu}{\kappa\cdot c_p}u^2 = \frac{\nu}{k\cdot c_p}\cdot\frac{kN(T_w - T_\infty)}{x\nu U_\infty}\frac{\nu}{k}U_\infty^2 f'^2(\eta) = N\frac{U_\infty}{x}(T_w - T_\infty)\cdot f'^2(\eta)$$

$$\frac{\sigma B_o^2}{\rho c_p}u^2 = \frac{\sigma B_o^2}{\rho c_p}(U_\infty f'(\eta))^2 = \frac{\sigma B_o^2}{\rho c_p}U_\infty^2 f'^2(\eta),\ \frac{Q_o}{\rho c_p}(T - T_\infty) = \frac{Q_o}{\rho c_p}(T_w - T_\infty)\theta(\eta)$$

Substituting the respective terms from into (3.63) yields;

$$-\frac{1}{2}\frac{U_\infty}{x}(T_w-T_\infty)\cdot\eta\cdot f'(\eta)\theta'(\eta)+\frac{1}{2}\frac{U_\infty}{x}(T_w-T_\infty)\cdot\eta\cdot f'(\eta)\theta'(\eta)-\frac{1}{2}\frac{U_\infty}{x}(T_w-T_\infty)f(\eta)\cdot\theta'(\eta)$$
$$=\frac{U_\infty}{x}\cdot\frac{1}{\Pr}(T_w-T_\infty)\cdot\theta''(\eta)+Ec(T_w-T_\infty)\frac{U_\infty}{x}f''^2(\eta)+N(T_w-T_\infty)\frac{U_\infty}{x}f'^2(\eta)+\frac{\sigma B_o^2}{\rho c_p}U_\infty^2 f'^2(\eta)+\frac{Q_o}{\rho c_p}(T_w-T_\infty)\theta(\eta)$$

Simplifying and multiplying through by $\frac{x\Pr}{U_\infty(T_w-T_\infty)}$ results in;

$$-\frac{1}{2}\Pr\cdot f(\eta)\cdot\theta'(\eta)=\theta''(\eta)+Ec\cdot\Pr\cdot f''^2(\eta)+N\cdot\Pr\cdot f'^2(\eta)+\frac{\sigma B_o^2 x}{\rho c_p}\frac{U_\infty^2}{U_\infty(T_w-T_\infty)}\Pr f'^2(\eta)+\frac{Q_o}{\rho c_p}\frac{x\Pr}{U_\infty}\theta(\eta)$$

But, $M=\frac{\sigma B_o^2\cdot x}{\rho U_\infty}, Ec=\frac{U_\infty^2}{c_p(T_w-T_\infty)}, bx=U_\infty, Q=\frac{Q_o x}{\rho c_p U_\infty}, \Pr=\frac{\upsilon}{\alpha}$

Substituting respective terms yields;

$$\theta''+\frac{1}{2}\cdot\Pr\cdot f\cdot\theta'+Q\cdot\Pr\cdot\theta+Ec\cdot\Pr\cdot f''^2+N\cdot\Pr\cdot f'^2+\Pr\cdot Ec\cdot Mf'^2=0 \quad (3.73)$$

3.7.4 Dimensionless Concentration Equation

The terms of the concentration equation 3.67 are transformed using the selected similarity variables. From the dimensionless quantity $\phi(\eta)=\frac{C-C_\infty}{C_w-C_\infty}$.

$$C=\phi(\eta)(C_w-C_\infty)+C_\infty$$

Differentiating with respect to x using the chain rule gives:

$$\frac{\partial C}{\partial x}=-\frac{1}{2}x^{-3/2}y\sqrt{\left(\frac{U_\infty}{\upsilon}\right)}\cdot\phi'(\eta)\cdot(C_w-C_\infty)=-\frac{1}{2}\frac{y}{x}\sqrt{\frac{U_\infty}{\nu x}}(C_w-C_\infty)\cdot\phi'(\eta)$$

Multiplying u by $\frac{\partial C}{\partial x}$ results in;

$$u\frac{\partial C}{\partial x} = -\frac{1}{2}\frac{y}{x}\sqrt{\frac{U_\infty}{\nu x}}(C_w - C_\infty)\cdot U_\infty f'\cdot\phi'(\eta) = -\frac{1}{2}\frac{U_\infty}{x}\cdot\eta\cdot(C_w - C_\infty)f'\cdot\phi'(\eta)$$

Similarly, differentiating with respect to y using the chain rule, we have;

$$\frac{\partial C}{\partial y} = \sqrt{\left(\frac{U_\infty}{\upsilon x}\right)}\cdot(C_w - C_\infty)\cdot\phi'$$

$$\frac{\partial^2 C}{\partial y^2} = \frac{\partial}{\partial y}\left(\sqrt{\left(\frac{U_\infty}{\upsilon x}\right)}\cdot(C_w - C_\infty)\cdot\phi'\right) = (C_w - C_\infty)\frac{U_\infty}{\upsilon x}\phi''(\eta)$$

Multiplying v by $\frac{\partial C}{\partial y}$ results in;

$$v\frac{\partial C}{\partial y} = \frac{1}{2}\sqrt{\frac{\nu U_\infty}{x}}[\eta\cdot f'(\eta) - f(\eta)]\cdot\sqrt{\left(\frac{U_\infty}{\nu x}\right)}\cdot(C_w - C_\infty)\cdot\phi'$$

$$v\frac{\partial C}{\partial y} = \frac{1}{2}\frac{U_\infty}{x}\eta(C_w - C_\infty)f'(\eta)\cdot\phi'(\eta) - \frac{1}{2}\frac{U_\infty}{x}(C_w - C_\infty)f(\eta)\phi(\eta)$$

$C - C_\infty = \phi(\eta)(C_w - C_\infty)$, and $\gamma(C - C_\infty) = \gamma\cdot(C_w - C_\infty)\cdot\phi(\eta)$

Substituting respective terms into equation 3.67 leads to:

$$-\frac{1}{2}\frac{U_\infty}{x}\cdot\eta\cdot(C_w - C_\infty)f'\cdot\phi'(\eta) + \frac{1}{2}\frac{U_\infty}{x}\eta(C_w - C_\infty)f'(\eta)\cdot\phi'(\eta) -$$
$$\frac{1}{2}\frac{U_\infty}{x}(C_w - C_\infty)f(\eta)\phi(\eta) = D\cdot(C_w - C_\infty)\frac{U_\infty}{\upsilon x}\phi''(\eta) - \gamma\cdot(C_w - C_\infty)\cdot\phi(\eta)$$

Simplifying, $-\frac{1}{2}\frac{U_\infty}{x}(C_w - C_\infty)f(\eta)\phi(\eta) = D\cdot(C_w - C_\infty)\frac{U_\infty}{\upsilon x}\phi''(\eta) - \gamma\cdot(C_w - C_\infty)\cdot\phi(\eta)$

$$\phi''(\eta)+\frac{1}{2}\frac{v}{D}f(\eta)\phi(\eta)-\frac{vx}{U_\infty}\frac{\gamma}{D}\cdot\cdot\phi(\eta)=0$$

$$\phi''(\eta)+\frac{1}{2}Sc\cdot f(\eta)\cdot\phi'(\eta)-\beta Sc\phi(\eta)=0 \qquad (3.74)$$

where $Sc=\frac{v}{D}$ and $\beta=\frac{\gamma x}{U_\infty}$

Hence equation 3.74 is the required dimensionless form of the concentration equation.

3.7.5 Dimensionless Boundary Conditions

The boundary conditions are transformed as follows.

Given that, $u(x,0)=0$, from (3.73), $u=U_\infty\cdot f'(\eta)$ and $\eta=y\sqrt{\frac{U_\infty}{vx}}$.

When y = 0, $\eta=0$, $\Rightarrow U_\infty\cdot f'(0)=0$, $\quad\therefore f'(0)=0$

Given that, $v(x,0)=0$, and $v=\frac{1}{2}\sqrt{\frac{vU_\infty}{x}}[\eta f'(\eta)-f(\eta)]$ as in (3.74);

When y = 0, $\Rightarrow\eta=0$ and v = 0, substituting into (3.33) we have;

$$0=\frac{1}{2}\sqrt{\frac{vU_\infty}{x}}[(0)f'(0)-f(0)], \qquad \Rightarrow f(0)=0$$

Considering the third boundary condition given as $-\kappa\frac{\partial T}{\partial y}=h_f\left[T_f-T(x,0)\right]$

$$\frac{\partial T}{\partial y}=(T_w-T_\infty)\cdot\sqrt{\frac{U_\infty}{vx}}\cdot\theta'(\eta),$$

Multiply both sides of (3.85) by - k and equating the results to $h_f\lfloor T_f - T(x,0)\rfloor$;

$$-k\frac{\partial T}{\partial y} = -k(T_w - T_\infty)\cdot\sqrt{\frac{U_\infty}{\nu x}}\cdot\theta'(\eta)$$

$$-k(T_w - T_\infty)\cdot\sqrt{\frac{U_\infty}{\nu x}}\cdot\theta'(\eta) = h_f\left[T_f - T(x,0)\right]$$

$$\theta'(\eta) = \frac{h_f}{k}\sqrt{\frac{\nu x}{U_\infty}}\frac{\lfloor T(x,0) - T_f\rfloor}{(T_w - T_\infty)}, \Rightarrow \theta'(\eta) = \frac{h_f}{k}\sqrt{\frac{\nu x}{U_\infty}}\cdot\frac{(T - T_\infty) - (T_w - T_\infty)}{T_w - T_\infty}$$

$$\therefore \theta'(\eta) = \frac{h_f}{k}\sqrt{\frac{\nu x}{U_\infty}}\cdot\frac{(T - T_\infty)}{T_w - T_\infty} - \frac{(T_w - T_\infty)}{T_w - T_\infty},$$

But $Bi_x = \frac{h_f}{k}\sqrt{\left(\frac{\upsilon x}{u_\infty}\right)}$ and $\theta(0) = \frac{(T - T_\infty)}{T_w - T_\infty}$,

$$\therefore \theta'(0) = B_{ix}\left[\theta(0) - 1\right]$$

Transforming the fourth boundary condition, $C(x,0) = C_w$;

$y = 0, \Rightarrow \eta = 0$ and substituting into $\phi(\eta) = \frac{C - C_\infty}{C_w - C_\infty}$ we have;

$$\phi(0) = \frac{C_w(x,0) - C_\infty}{C_w - C_\infty} = \frac{C_w - C_\infty}{C_w - C_\infty} = 1, \qquad \therefore \phi(0) = 1$$

Transforming the fifth boundary condition, $u(x,\infty) = U_\infty$ as $y \to \infty, \Rightarrow \eta \to \infty$

Substituting into $u = U_\infty f'(\eta)$, $U_\infty = U_\infty f'(\infty) \Rightarrow f'(\infty) = \frac{U_\infty}{U_\infty} = 1$, $\therefore f'(\infty) = 1$

Transforming the sixth boundary condition, $T(x,\infty)=T_\infty$ using $\theta(\eta)=\dfrac{T-T_\infty}{T_w-T_\infty}$;

When $y\to\infty,\Rightarrow\eta\to\infty$ and $T\to T_\infty$, $\Rightarrow\theta(\infty)=\dfrac{T_\infty-T_\infty}{T_w-T_\infty}=0$, $\therefore\theta(\infty)=0$.

Transforming the seventh boundary condition, $C(x,\infty)=C_\infty$ using $\phi(\eta)=\dfrac{C-C_\infty}{C_w-C_\infty}$;

As $y\to\infty,\Rightarrow\eta\to\infty$ and $C\to C_\infty$ $\Rightarrow\phi(\infty)=\dfrac{C_\infty-C_\infty}{C_w-C_\infty}=0$ $\therefore\phi(\infty)=0$

It is noticed that the local parameters B_i, Gr, Gc and B are all functions of x. However in order to have similarity solution all parameters must be constant and we therefore make the following assumptions $h_f=ax^{-1/2}$, $\beta_T=bx^{-1}$, $\beta_C=cx^{-1}$ and $\gamma=dx^{-1}$ where a, b, c and d are constants.

At the surface of the plate $\eta=0$, $u=0$, $v=0$, $C=C_w$ and $T=T_w$

Thus, $f'(0)=0$, $f(0)=0$, $\phi(0)=1$, $\theta(0)=1$,

As $\eta\to\infty$, $f'(\infty)=1$, $\theta(\infty)=0$, $\phi(\infty)=0$ (3.75)

3.7.6 Reduction of Order

The third order nonlinear ordinary differential equations are reduced to a system of first order ordinary differential equations to enable direct solutions;

Let $x_1=f(\eta)$, $x_2=f'(\eta)$ and $x_3=f''(\eta)$.

$\Rightarrow x_1' = f'(\eta) = x_2$, $x_2' = f''(\eta) = x_3$ and $x_3' = f'''(\eta)$.

Let $y_1 = \theta(\eta)$ and $y_2 = \theta'(\eta)$ $\Rightarrow y_1' = \theta'(\eta) = y_2$, $y_2' = \theta''(\eta)$.

Let $z_1 = \phi(\eta)$ and $z_2 = \phi'(\eta)$ $\Rightarrow z_1' = \phi'(\eta) = z_2$ and $z_2' = \phi''(\eta)$.

Hence the required first order system is;

$$
\begin{aligned}
x_1' &= x_2 \\
x_2' &= x_3 \\
x_3' &= -\frac{1}{2}x_1 \cdot x_3 - Gr \cdot y_1 \sin(\alpha) - Gc \cdot z_1 \sin(\alpha) + (\delta + M) \cdot x_2 - \delta \\
y_1' &= y_2 \\
y_2' &= -\frac{1}{2}\Pr \cdot x_1 \cdot y_2 - Q \cdot \Pr \cdot y_1 - Ec \cdot \Pr \cdot x_3^2 - N \cdot \Pr \cdot x_2^2 - \Pr \cdot Ec \cdot M \cdot x_2^2 \\
z_1' &= z_2 \\
z_2' &= -\frac{1}{2}Sc \cdot x_1 \cdot z_2 + \beta \cdot Sc \cdot z_1
\end{aligned}
\qquad (3.76)
$$

The corresponding boundary conditions are obtained as;

When $\eta = 0$, $u = 0$, $v = 0$, $C = C_w$ and $T = T_w$

$x_1(0) = 0$, $x_2(0) = 0$, $z_1(0) = 1$, $y_2(0) = Bi \cdot (y_1(0) - 1)$, $x_3(0) = s_1$, $y_1(0) = s_2$, $z_2(0) = s_3$

As $\eta \to \infty$, $x_2(\infty) = 1$, $y_1(\infty) = 0$, $z_1(\infty) = 0$ (3.77)

This first order system of differential equations 3.76 along with the boundary conditions 3.77 shall be coded using the 4th order Runge-Kutta algorithm with the shooting method to obtain relevant results for analysis in the next chapter.

CHAPTER FOUR

4.0 RESULTS AND DISCUSSIONS

4.1 Introduction

The transformed dimensionless nonlinear ordinary differential equations with boundary conditions are solved with Maple 16 using the fourth-order Runge-Kutta method. Numerical results are tabulated increasing values of various controlling parameters and discussed. Graphical illustrations of the results have also been given for velocity, temperature and concentration profiles in the boundary layer region.

4.2 Numerical Results and Discussions

The transformed third order ordinary differential equations were reduced to a system of first order ordinary differential equations and simulated under similar conditions to previously published work of Makinde and Olanrewaju (2010). A comparison of results showed an excellent agreement validating the procedure,(see Table 4.1). Similar observations were made when compared with Makinde (2010) in Table 4.2, validating the procedure.

Table 4.1: Comparison of $f''(0)$, $-\theta'(0)$ and $\theta(0)$ for values of Bi, Gr and Pr when $\beta = Q = N = Ec = \delta = M = 0$ and $\alpha = \pi/2$

			Makinde and Olanrewaju (2010)			Present Results		
Bi	Gr	Pr	$f''(0)$	$-\theta'(0)$	$\theta(0)$	$f''(0)$	$-\theta'(0)$	$\theta(0)$
0.1	0.1	0.72	0.36881	0.07507	0.24922	0.368816	0.075077	0.249228
1.0	0.1	0.72	0.44036	0.23750	0.76249	0.440365	0.237506	0.762494
10.0	0.1	0.72	0.46792	0.30559	0.96944	0.467928	0.305596	0.969440
0.1	0.5	0.72	0.49702	0.07613	0.23862	0.497022	0.076138	0.238623
0.1	1.0	0.72	0.63200	0.07704	0.22955	0.632007	0.077045	0.229552
0.1	0.1	3.00	0.34939	0.08304	0.16954	0.349397	0.083046	0.169540
0.1	0.1	7.10	0.34270	0.08672	0.13278	0.342705	0.086721	0.132788

Table 4.2: Comparison of $f''(0)$, $-\theta'(0)$, $\theta(0)$ and $-\phi'(0)$ for values of Bi, Gr, Gc, Pr and Sc when $\beta = Q = N = Ec = \delta = 0$ and $\alpha = \pi/2$.

						Makinde (2010)			Present Results		
Bi	Gr	Gc	Ha	Pr	Sc	$f''(0)$	$-\theta'(0)$	$-\phi'(0)$	$f''(0)$	$-\theta'(0)$	$-\phi'(0)$
0.1	0.1	0.1	0.1	0.72	0.62	-0.40227	0.07864	0.33374	-0.40227	0.07864	0.33374
1.0	0.1	0.1	0.1	0.72	0.62	-0.35214	0.27315	0.34103	-0.35214	0.27315	0.34103
0.1	0.5	0.1	0.1	0.72	0.62	-0.32221	0.07917	0.34513	-0.32221	0.07917	0.34513
0.1	1.0	0.1	0.1	0.72	0.62	-0.23125	0.07969	0.35667	-0.23125	0.07969	0.35667
0.1	0.1	0.5	0.1	0.72	0.62	-0.02641	0.08071	0.38140	-0.02641	0.08071	0.38140
0.1	0.1	1.0	0.1	0.72	0.62	-0.37992	0.08204	0.41767	-0.37992	0.08204	0.41767
0.1	0.1	0.1	0.5	0.72	0.62	-2.21793	0.06616	0.18066	-2.21793	0.06616	0.18066
0.1	0.1	0.1	1.0	0.72	0.62	-0.43079	0.08194	0.33252	-0.43079	0.08194	0.33252
0.1	0.1	0.1	0.1	1.00	0.62	-0.42123	0.09335	0.33056	-0.42123	0.09335	0.33056
0.1	0.1	0.1	0.1	7.10	0.62	-0.44170	0.07848	0.38446	-0.44170	0.07848	0.38446
0.1	0.1	0.1	0.1	0.72	0.78	-0.45309	0.07792	0.79815	-0.45309	0.07792	0.79815

The effects of increasing parameter on the skin friction coefficient, Nusselt number and Sherwood numbers as well as plate surface temperature are numerically displayed in Tables 4.3 and 4.4. From Table 4.3, it is observed that increasing the Biot number (Bi) from 0.1 to 1.0 resulted in an increase in the skin friction coefficient from 2.119394 to 2.163412 but decreased the Nusselt from - 0.048412 to - 0.154048 and Sherwood numbers from - 0.429002 to - 0.430830. Thus, increasing the Biot number implies an increase in the heat transfer coefficient which enhances buoyancy in the boundary layer. Agitated fluid molecules on the surface of the plate increased the friction coefficient thereby increasing the plate surface temperature from 0.515880 to 0.845952 as shown in Table 4.3.

It is also observed that increasing the angle of inclination from 0^o to 90^o has a dual effect of decreasing or increasing the temperature and skin friction coefficient in the boundary layer. From Table 4.3, it can be observed that increasing the angle of inclination from 0^o to 10^o decrease the temperature of the plate from 0.518299 to

0.515214 and above 10^o caused an increase in the plate's temperature from 0.515214 to 0.519434. However increased angle of inclination generally resulted in decreasing Sherwood number from - 0.419191 to - 0.462569 as depicted in Table 4.3.

Table 4.3: Effect of Parameter Variations on Heat and Mass Transfer Rate for Pr = 0.72, Ec = 0.02, Q = 0. 1, Gr = 3.2, Gc = 3.5 and Sc = 0.6

Bi	α	M	β	N	δ	$f''(0)$	$-\theta'(0)$	$\theta(0)$	$-\phi'(0)$
0.1	$\pi/30$	0.5	0.1	0.04	4.0	2.119394	0.048412	0.515880	0.429002
0.5	$\pi/30$	0.5	0.1	0.04	4.0	2.150929	0.123875	0.752251	0.430313
1.0	$\pi/30$	0.5	0.1	0.04	4.0	2.163412	0.154048	0.845952	0.430830
0.1	0.0	0.5	0.1	0.04	4.0	1.901360	0.048170	0.518299	0.419191
0.1	$\pi/30$	0.5	0.1	0.04	4.0	2.119394	0.048412	0.515880	0.429002
0.1	$\pi/18$	0.5	0.1	0.04	4.0	2.262447	0.048479	0.515214	0.435235
0.1	$\pi/12$	0.5	0.1	0.04	4.0	2.437863	0.048475	0.515249	0.442676
0.1	$\pi/6$	0.5	0.1	0.04	4.0	2.931966	0.048057	0.519434	0.462569
0.1	$\pi/3$	0.5	0.1	0.04	4.0	2.931966	0.048057	0.519434	0.462569
0.1	$\pi/2$	0.5	0.1	0.04	4.0	2.931920	0.048057	0.519434	0.462569
0.1	$\pi/30$	1.0	0.1	0.04	4.0	2.017248	0.043801	0.561993	0.417651
0.1	$\pi/30$	1.5	0.1	0.04	4.0	1.930576	0.038817	0.611826	0.407795
0.1	$\pi/30$	2.5	0.1	0.04	4.0	1.790817	0.027950	0.720504	0.391478
0.1	$\pi/30$	0.5	0.2	0.04	4.0	2.116495	0.048404	0.515962	0.486312
0.1	$\pi/30$	0.5	0.3	0.04	4.0	2.113918	0.048397	0.516034	0.538941
0.1	$\pi/30$	0.5	0.4	0.04	4.0	2.111599	0.048390	0.516610	0.587781
0.1	$\pi/30$	0.5	0.1	0.16	4.0	2.212897	-0.009115	1.091146	0.434583
0.1	$\pi/30$	0.5	0.1	0.20	4.0	2.244744	-0.028719	1.287192	0.436453
0.1	$\pi/30$	0.5	0.1	0.24	4.0	2.276940	-0.048544	1.485442	0.438329
0.1	$\pi/30$	0.5	0.1	0.04	4.5	2.236181	0.048301	0.516986	0.431744
0.1	$\pi/30$	0.5	0.1	0.04	5.0	2.346934	0.048192	0.518082	0.434132
0.1	$\pi/30$	0.5	0.1	0.04	6.0	2.553597	0.047978	0.520217	0.438119

The effect of variation of angle of inclination on the skin friction coefficient is observed in Table 4.3. Between 0^o and 60^o the skin friction increased from 1.901360 to 2.931966 and decreased from 2.931966 to 2.931920 for angles from 60^0 to 90^0. Increasing the magnetic field parameter from 1.0 to 2.5 caused a decrease in the skin friction coefficient from 2.017248 to 1.790817 but increased the temperature of the plate from 0.561993 to 0.720504 and Sherwood number from - 0.417651 to - 0.391478. The magnetic field produces a Lorenz force which retards the motion of the fluid and reduces the buoyancy causes an in increased Nusselt number from -0.043801 to - 0.027950 and Sherwood number from -0.462569 to -0.391478, resulting in an increase in the temperature of the plate from 0.561993 to 0.720504 as shown in Table 4.3.

Table 4.4: Effect of Parameters Variation on Heat and Mass Transfer Rate for Bi = 0.1, $\alpha = \pi/30$, M=0.5, $\beta = 0.1$, N = 3.2, and δ = 4.

Pr	Ec	Sc	Gr	Gc	Q	$f''(0)$	$-\theta'(0)$	$\theta(0)$	$-\phi'(0)$
0.72	0.02	0.6	3.2	3.5	0.10	2.119394	0.048412	0.515880	0.429002
1.00	0.02	0.6	3.2	3.5	0.10	2.121602	0.046576	0.534239	0.429005
3.60	0.02	0.6	3.2	3.5	0.10	2.138888	0.031605	0.683949	0.429200
0.72	0.40	0.6	3.2	3.5	0.10	2.388417	-0.127549	2.275494	0.442892
0.72	0.80	0.6	3.2	3.5	0.10	2.707231	-0.340511	4.405112	0.457972
0.72	1.00	0.6	3.2	3.5	0.10	2.884466	-0.460915	5.609155	0.465809
0.72	0.02	1.2	3.2	3.5	0.10	2.109251	0.048375	0.516246	0.584786
0.72	0.02	1.4	3.2	3.5	0.10	2.106767	0.048366	0.516337	0.625958
0.72	0.02	1.6	3.2	3.5	0.10	2.104554	0.048358	0.516416	0.663802
0.72	0.02	0.6	3.5	3.5	0.10	2.126531	0.048416	0.515840	0.429368
0.72	0.02	0.6	4.0	3.5	0.10	2.138421	0.048422	0.515777	0.429978
0.72	0.02	0.6	7.0	3.5	0.10	2.209685	0.048447	0.515534	0.433602
0.72	0.02	0.6	3.2	4.0	0.10	2.139499	0.048427	0.515732	0.429808
0.72	0.02	0.6	3.2	4.5	0.10	2.159590	0.048440	0.515595	0.430611
0.72	0.02	0.6	3.2	7.0	0.10	2.259821	0.048492	0.515085	0.434581
0.72	0.02	0.6	3.2	3.5	0.20	2.154505	0.025975	0.740251	0.430842
0.72	0.02	0.6	3.2	3.5	0.25	2.184939	0.006484	0.935162	0.432413
0.72	0.02	0.6	3.2	3.5	0.30	2.232745	-0.024196	1.241959	0.434847

Increasing the chemical reaction parameter from 0.2 to 0.4 caused a decrease in the skin friction coefficient from 2.116495 to 2.111599 and the Sherwood number from -0.486312 to -0.587781 but increased the Nusselt number from 0.048404 to 0.048390, as in Table 4.3. As a result, the plate's temperature increased from 0.515962 to 0.516610 due to exothermic reaction and the shear stresses between fluid molecules and between fluid molecules and the plate surface. Increasing the viscous dissipation parameter from 0.16

to 0.24 caused an increase in the local skin friction coefficient from 2.212897 to 2.276940 and the local Nusselt number from 0.009115 to 0.048544, but decreases the local Sherwood number from -0.434583 to -0.438329. Increasing the porosity parameter from 4.5 to 6.0 increased the local skin friction coefficient from 2.236181 to 2.553597 and local Nusselt number from -0.048301 to -0.047978, but decreases the local Sherwood number from -0.431744 to -0.438119. The parameters are observed to decrease the local Sherwood number because both parameters enhance interaction between molecules of the fluid and the plate surface increasing shear stress and temperature of the plate as in Table: 4.3.

It is further observed that increasing the Prandtl number from 0.72 to 3.60 the skin friction coefficient increased from 2.119394 to 2.138888, the Nusselt number from -0.048412 to -0.031605, the plate's temperature from 0.515880 to 0.683949 and the Sherwood number from -0.429002 to -0.429200. Also increasing the Eckert number from 0.40 to 1.00, the skin friction coefficient increased from 2.388417 to 2.884466, the Nusselt number from 0.127549 to 0.460915, the plate's temperature from 2.275494 to 5.609155 and the Sherwood number decreased from -0.442892 to 0.465809.

However increasing the Schmidt number from 1.2 to 1.6 decreased the skin friction coefficient from 2.109251 to 2.104554, the Sherwood number from -0.584786 to -0.663802 and increased the Nusselt number from -0.048375 to -0.048358, the plate's temperature from 0.516246 to 0.516416. The increase in Schmidt number decreased the local skin friction coefficient and the Sherwood number, thereby shrinking the concentration boundary layer. However the increase in the Nusselt number thickens the thermal boundary layer as depicted numerically in Table 4.4.

Similarly, increasing the thermal Grashof number from 3.5 to 7.0 increased the skin friction coefficient from 2.126531 to 2.209685, decreased the Nusselt number from -0.048416 to -0.048447, the plate's temperature from 0.515840 to 0.515534 and the Sherwood number from -0.429368 to -0.433602 as in Table 4.4.

Furthermore, increasing the solutal Grashof number from 4.0 to 7.0 increased the skin friction coefficient from 2.139499 to 2.259821, decreased the Nusselt number from -0.048427 to -0.048492, the plate's temperature from 0.515732 to 0.515085 and the Sherwood number from -0.429808 to -0.434581. An increase in both Grashof numbers improves buoyancy and convection which enable fluid molecules to efficiently move away from the plate surface leading to reduction in temperature. However shear stresses between the energetic molecules and the surface of the inclined plate accounts for the increased skin friction coefficient.

In addition increasing the local heat generation parameter from 0.20 to 0.30 increased the skin friction coefficient from 2.154505 to 2.232745, the Nusselt number from -0.025975 to 0.024196, the temperature of the plate from 0.740251 to 1.241959 and decreased the Sherwood number from -0.430842 to -0.434847 as shown in Table 4.4.

The increase in Schmidt number decreased the local skin friction coefficient and the Sherwood number, thereby shrinking the concentration boundary layer. However the increase in the Nusselt number thickens the thermal boundary layer as depicted numerically in Table 4.4.

4.3 Graphical Results and Discussions

4.3.1 Effects of Parameter Variation on Velocity Profiles

The effects of parameter variation on the velocity profile in the boundary layer are shown below in Figures 4.1 - 4.10. It is observed in Figure 4.1 that increasing values of the angle of inclination tend to sharply increase the velocity of the fluid within the boundary layer. The effect of inclination enhanced the effect of gravity and buoyancy forces which resulted in increased velocity in the boundary layer. Also a significant increase in velocity is observed when the viscous dissipation, thermal Grashof, solutal Grashof, local heat generation, Eckert number, Biot number and porosity parameters are increased as depicted in Figures 4.2, 4.3, 4.4, 4.6, 4.7, 4.9 and 4.10 respectively. The increased velocity is as a result of the inclination and buoyancy forces. It also facilitates efficient transport and distribution of heat and mass.

It is also observed that increasing the Prandtl number and the magnetic parameter results in decreased velocity in the boundary layer of the fluid as displayed in Figure 4.2 and 4.6 respectively. The decreased velocity that is observed from the increase of the magnetic parameter resulted in the thickening of the thermal and concentration boundary layers.

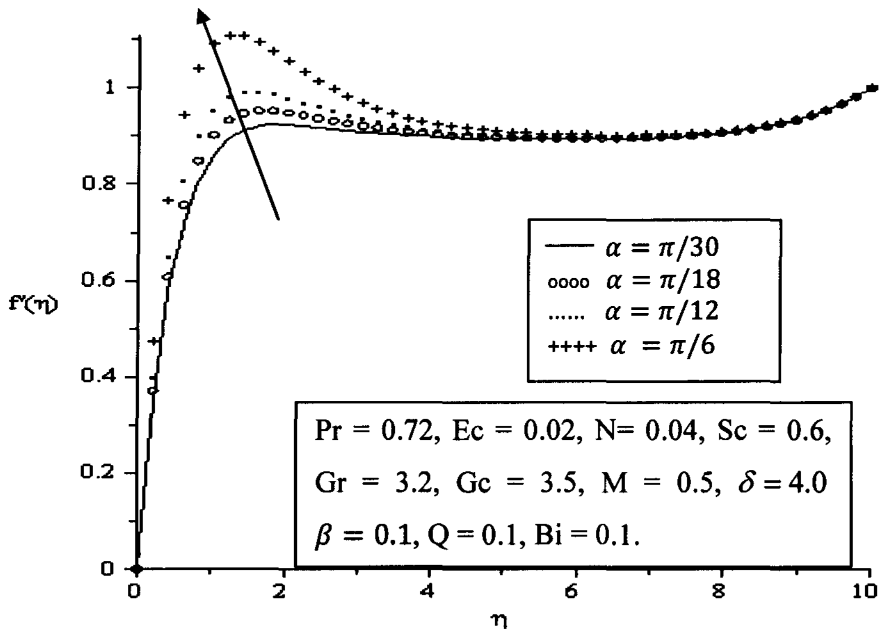

Figure 4.1: Effect of variation of angle of inclination (∝) on velocity profile.

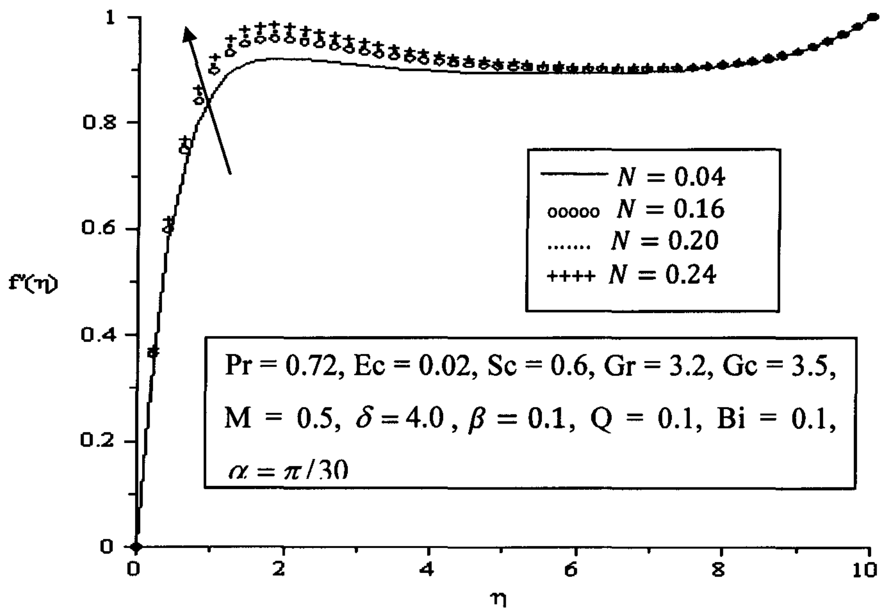

Figure 4.2: Effect of variation of viscous dissipation parameter (N) on velocity profile.

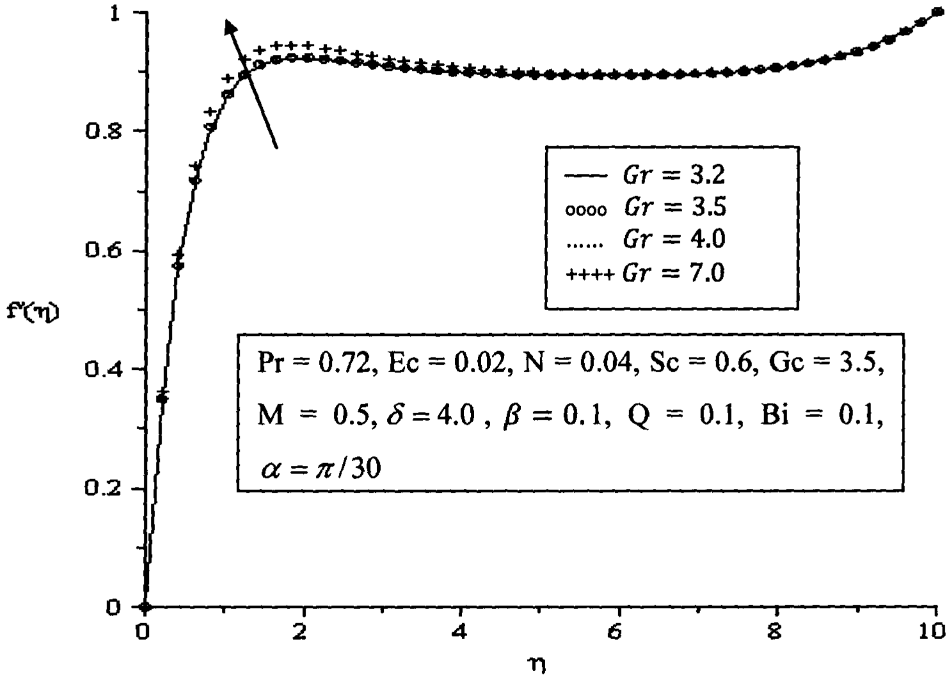

Figure 4.3: Effect of variation of thermal Grashof number (Gr) on velocity profile.

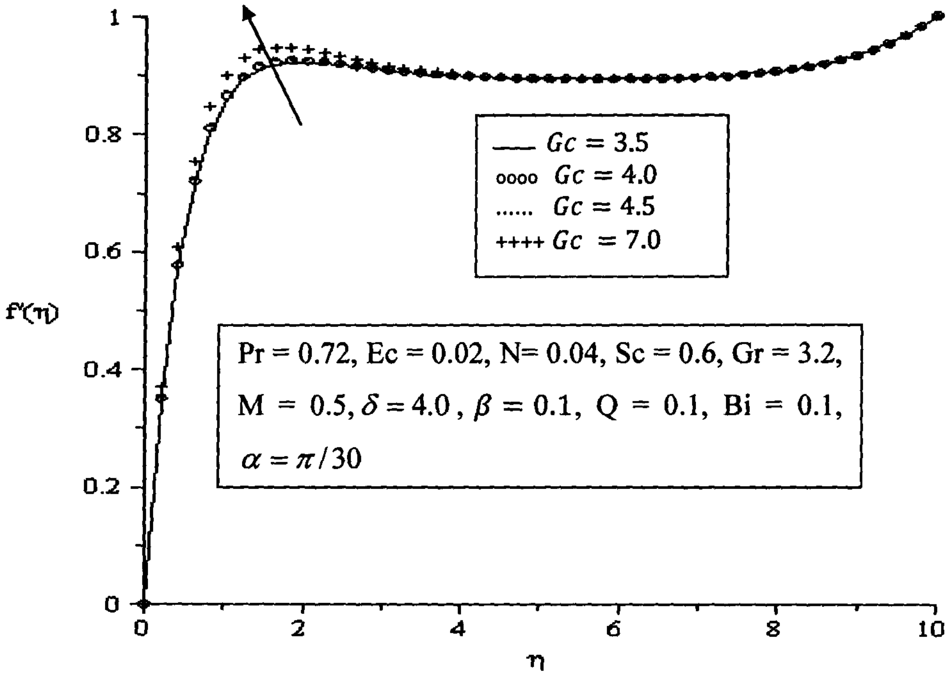

Figure 4.4: Effect of variation of solutal Grashof number (Gc) on velocity profile.

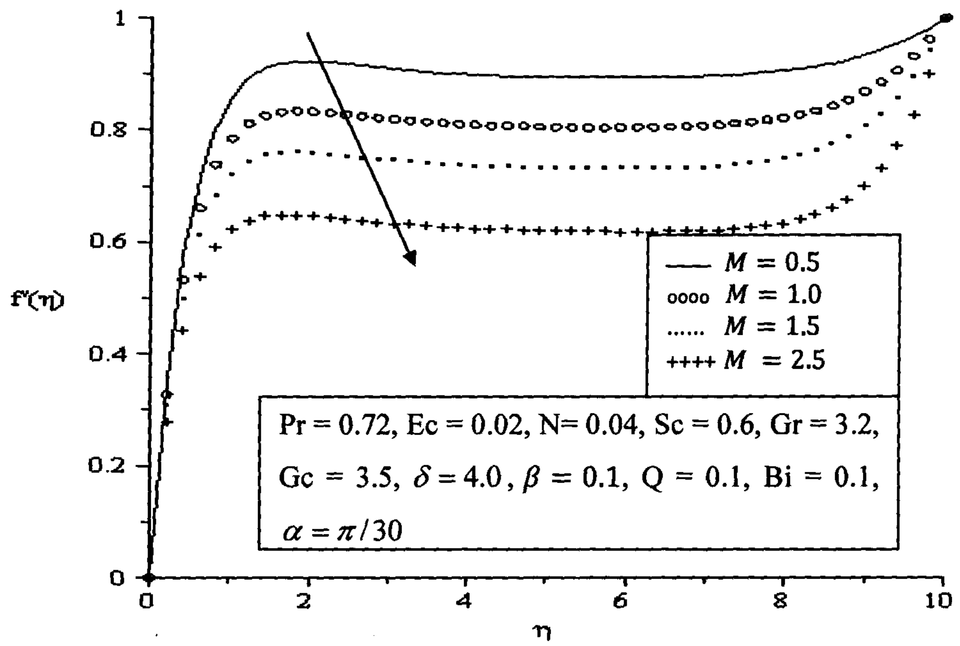

Figure 4.5: Effect of variation of Magnetic Parameter (M) on velocity profile.

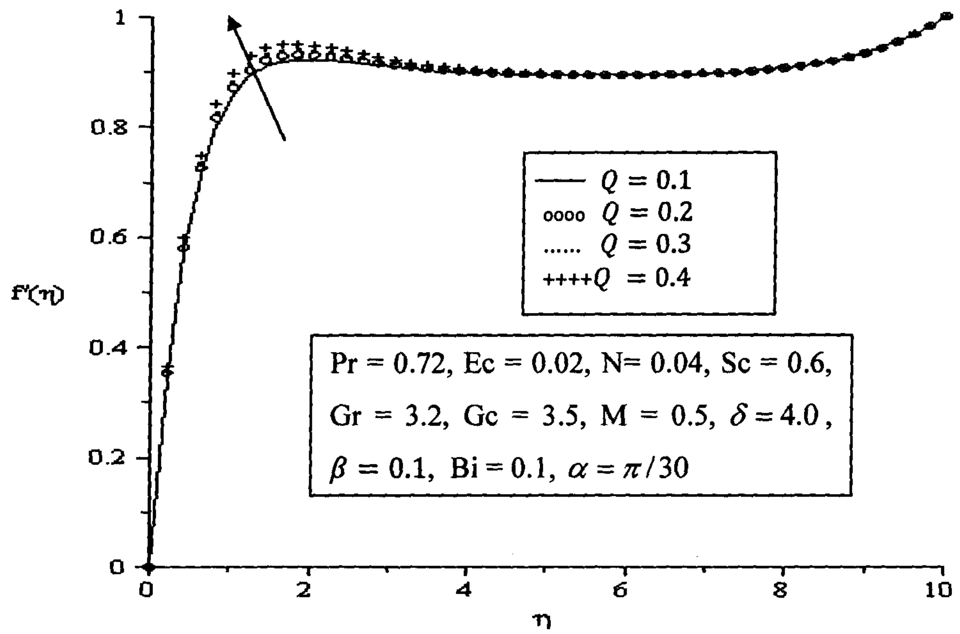

Figure 4.6: Effect of variation of Local heat source parameter (Q) on velocity profile.

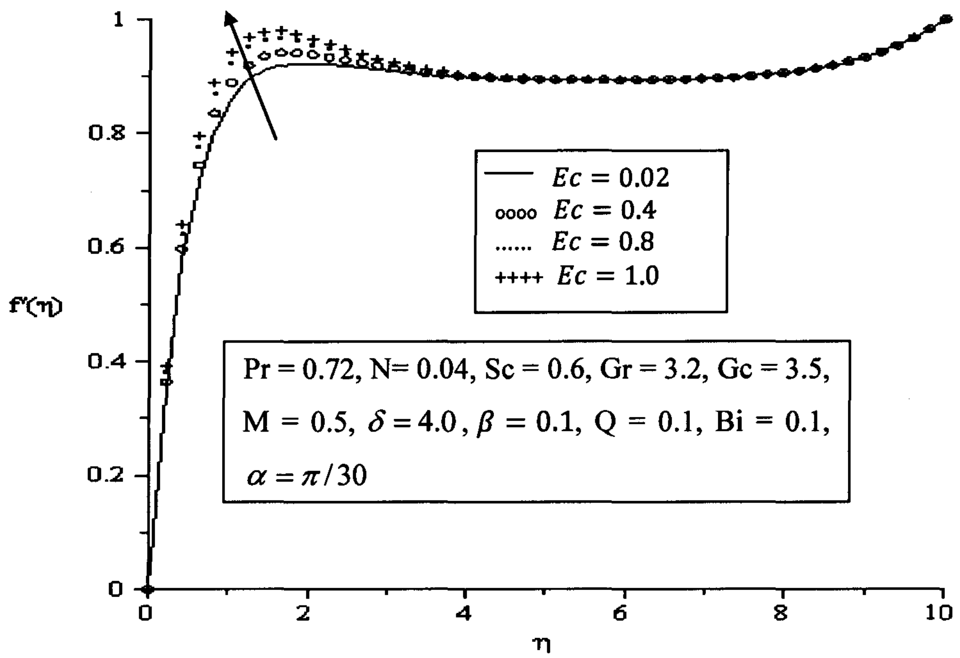

Figure 4.7: Effect of variation of Eckert number (Ec) on velocity profile.

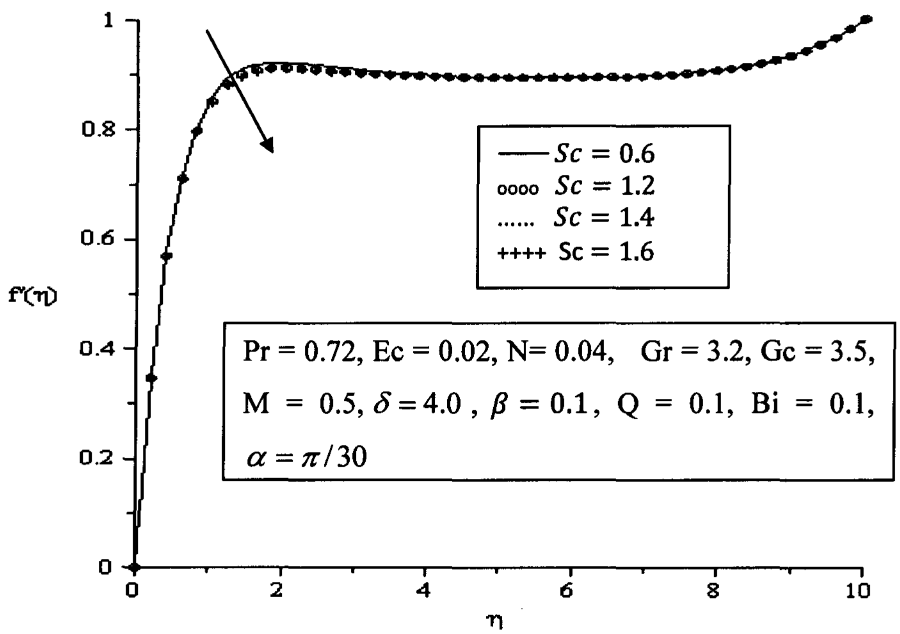

Figure 4.8: Effect of variation of Schmidt number (Sc) on velocity profile.

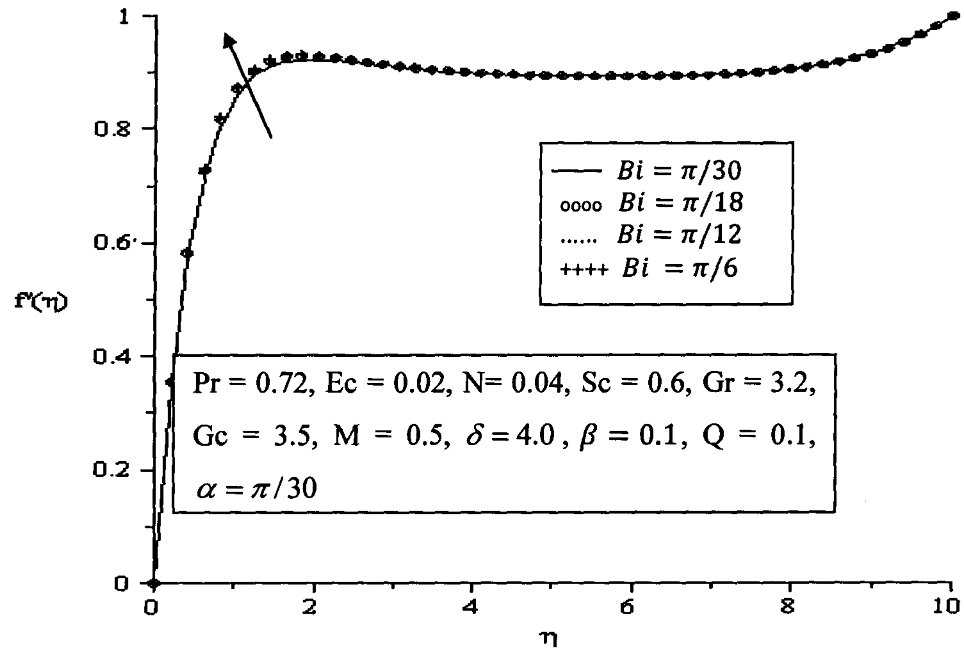

Figure 4.9: Effect of variation of Biot number (Bi) on velocity profile.

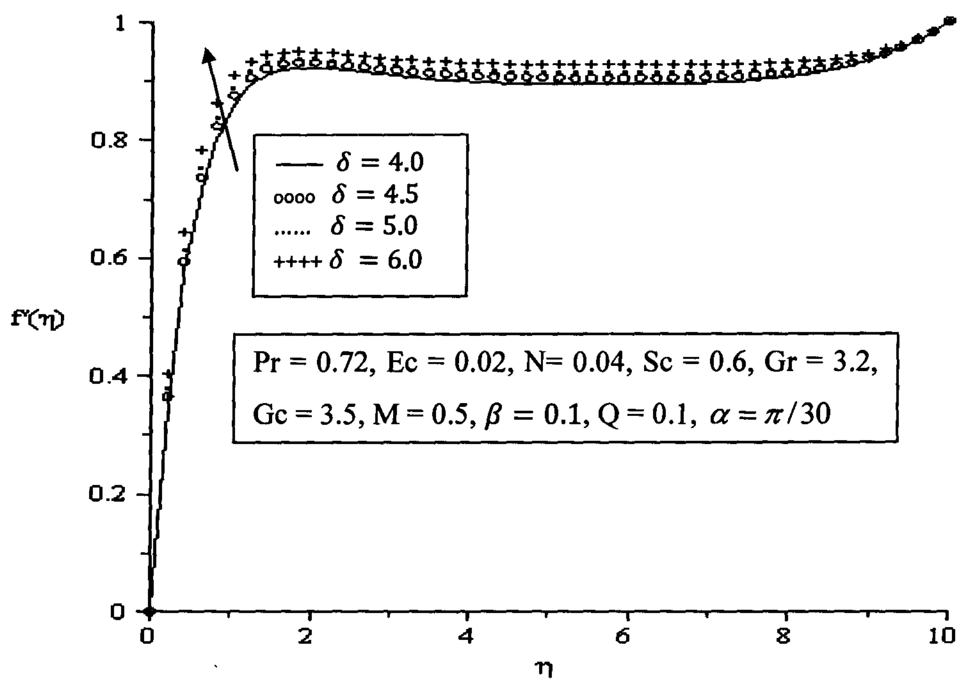

Figure 4.10: Effect of variation of Porosity (δ) on velocity profile.

4.3.2 Effects of Parameter Variation on Temperature Profiles

The effects of parameters variation on the temperature profile are shown in Figures 4.11 - 4.17. Increasing the angle of inclination causes a decrease in temperature as graphically displayed in Figure 4.11. The temperature drop resulted from the increased velocity which enhanced convection and heat dissipation. We also observed in Figure 4.12 that increasing the value of the Prandtl number decreases the temperature in the boundary layer. The combined effects of inclination and buoyancy forces significantly contributed to the resultant decreased temperature in the boundary layer. It is also observed that increasing the Eckert number, viscous dissipation parameter, Schmidt number, local heat generation parameter and Biot number resulted in increased temperature as depicted in Figures 4.12 – 4.17 respectively. In Figure 4.14 and 4.16, it is observed that increasing both the viscous dissipation and the local heat generation parameters, significantly increases the thickness of the thermal boundary layer.

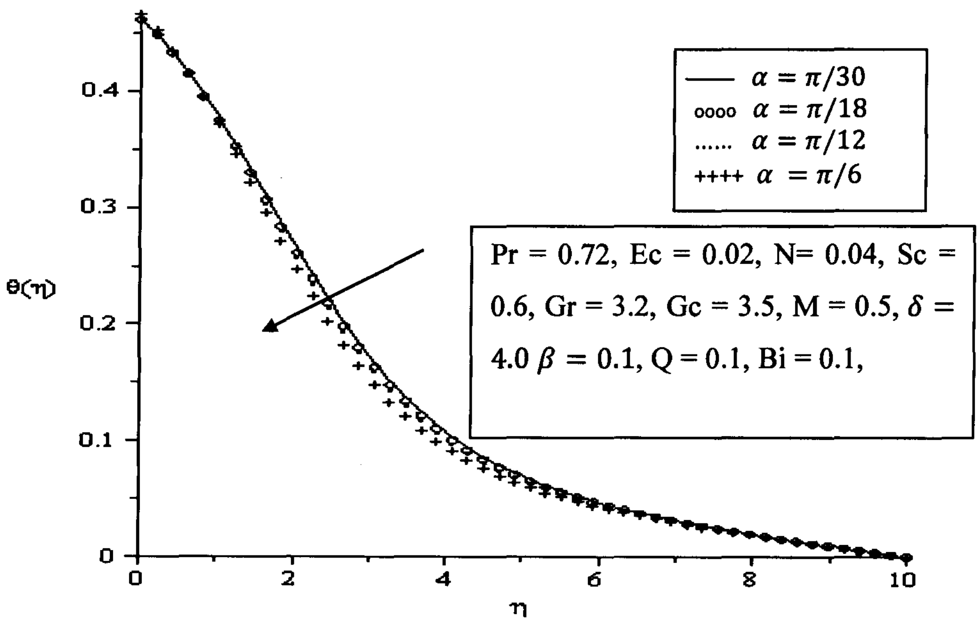

Figure 4.11: Effect of variation of angle of inclination (∝) on Temperature profile.

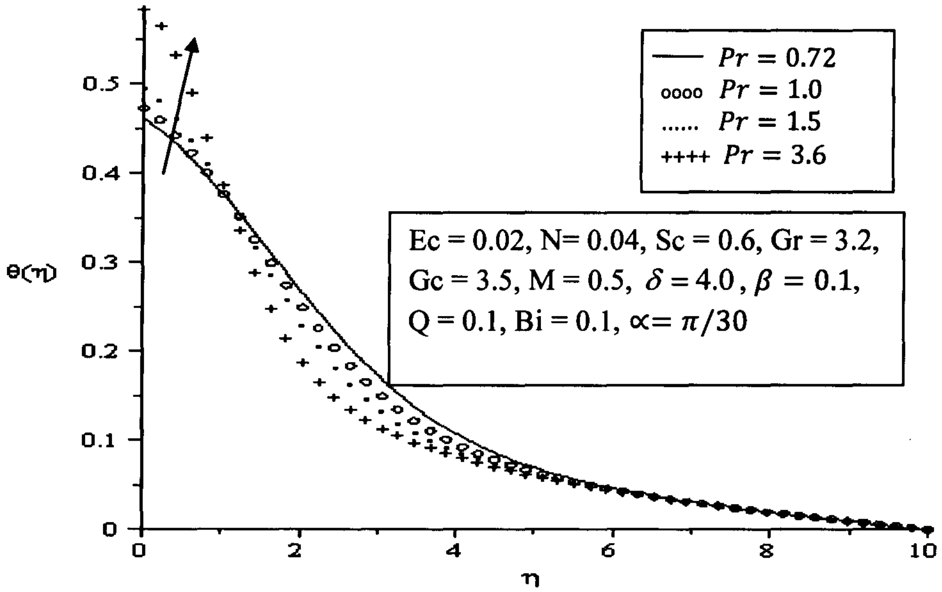

Figure 4.12: Effect of variation of Prandtl number (Pr) on Temperature profile.

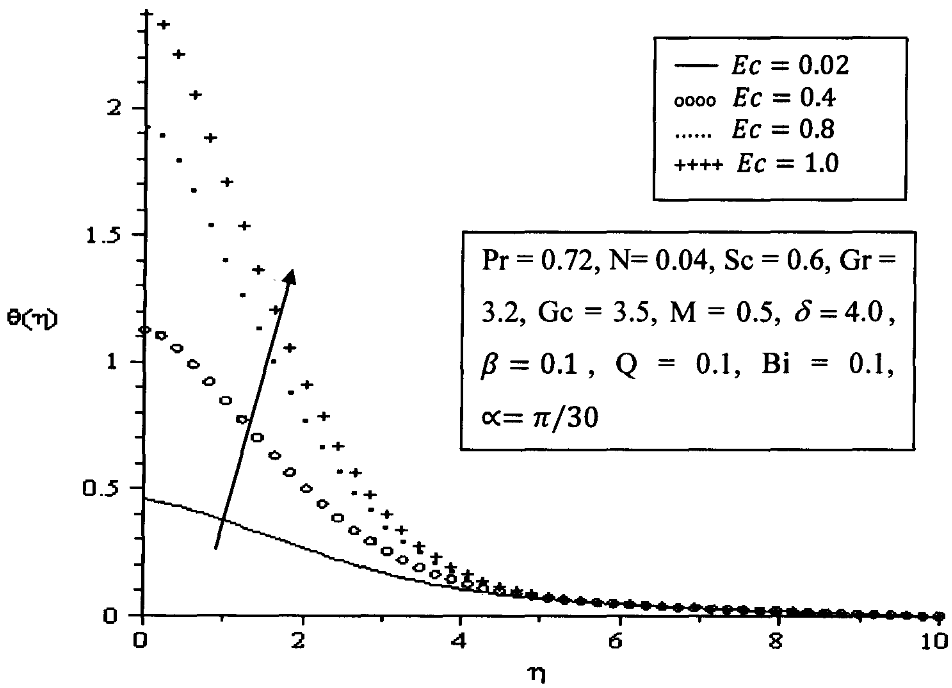

Figure 4.13: Effect of variation of Eckert number on Temperature profile.

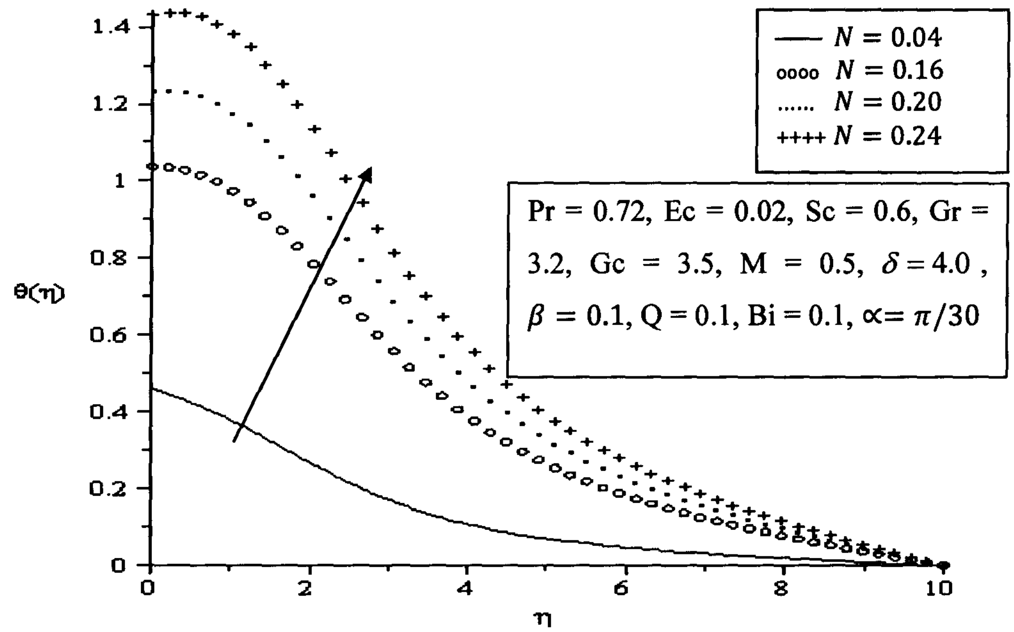

Figure 4.14: Effect of variation of viscous dissipation parameter (N) on Temperature profile.

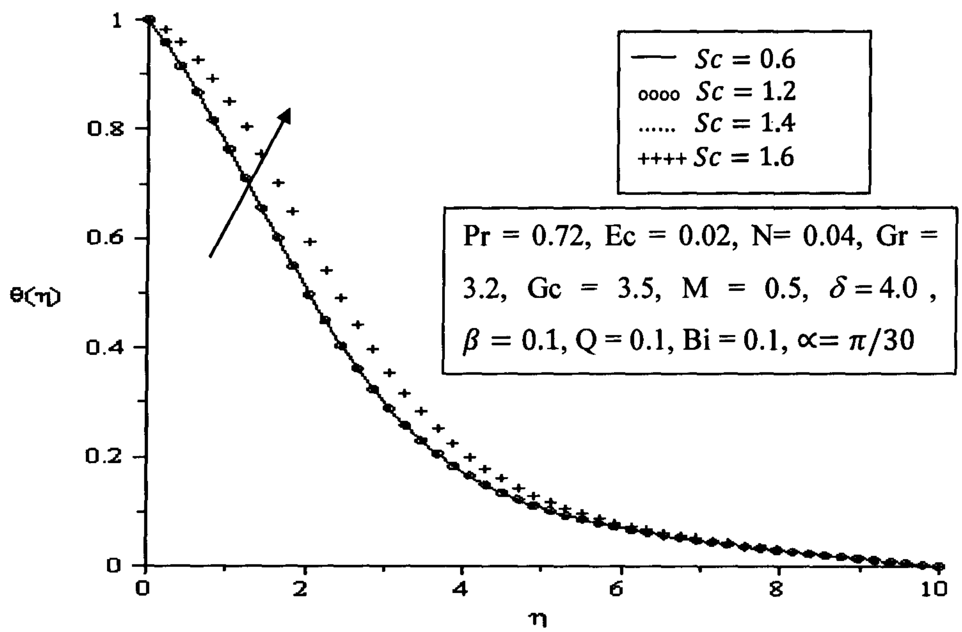

Figure 4.15: Effect of variation of Schmidt number (Sc) on Temperature profile.

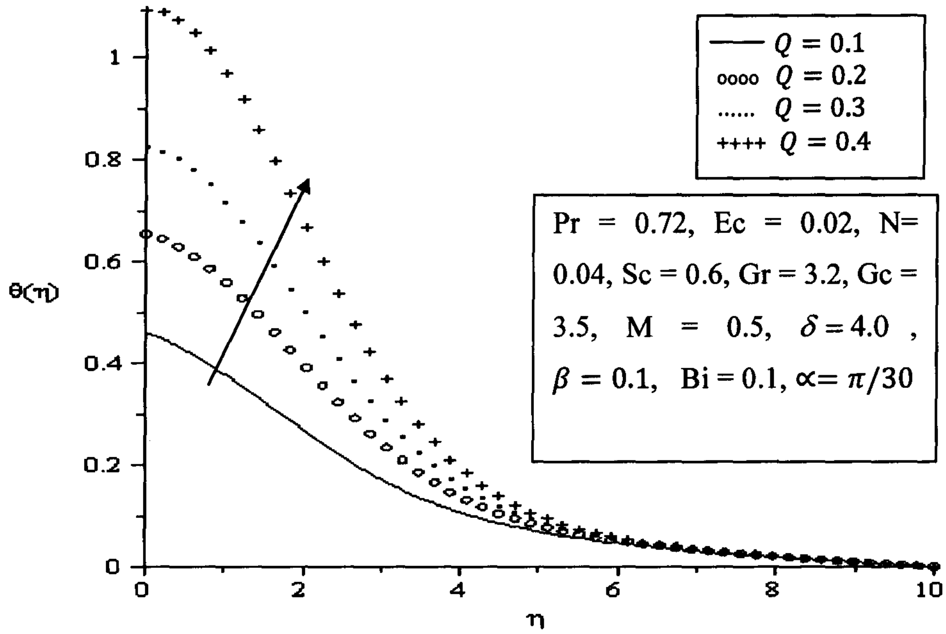

Figure 4.16: Effect of variation of Local heat generation parameter (Q) on Temperature profile.

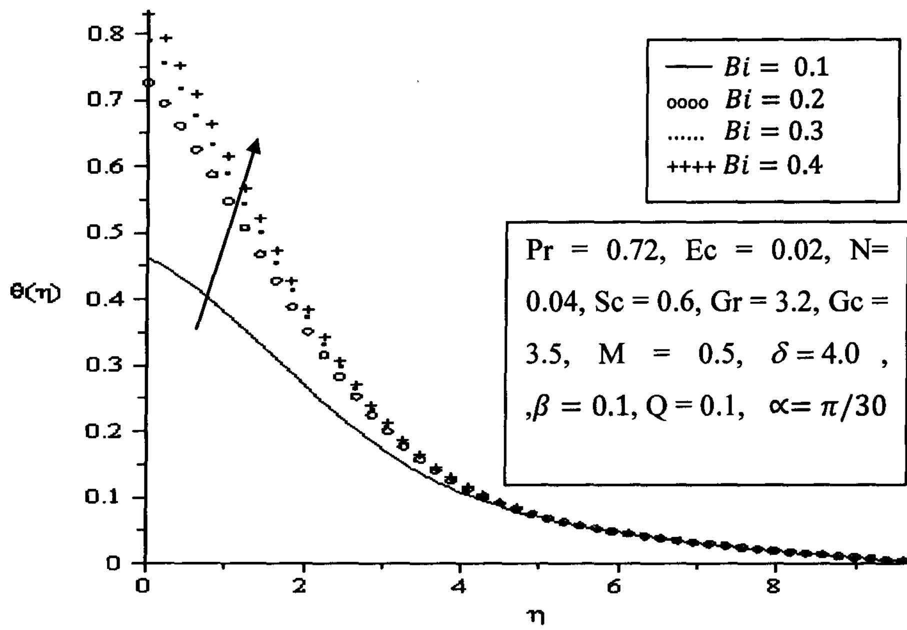

Figure 4.17: Effect of variation of Biot number (Bi) on Temperature profile.

4.3.3 Effects of Parameter Variation on Concentration Profiles

Figures 4.18 - 4.21 depict the effects of variation of parameters on the thickness of the concentration boundary layer. A reduction in thickness of the concentration boundary layer is observed upon increasing the angle of inclination, Schmidt number and Chemical reaction parameter as displayed in Figures 4.18, 4.19 and 4.21 respectively. The decay of the thickness of the concentration boundary layer is as a result of increased velocity and molecular diffusion. The thinning of the concentration boundary layer indicates efficient transport of mass of fluid. However we observed an increase in the concentration boundary layer when the magnetic parameter is increased as graphically displayed in Figure 4.20. The Lorenz force produced by the magnetic field retard free convective transfer of fluid mass leaving some molecules stack to the surface of the plate, resulting in the thickening of the concentration boundary layer.

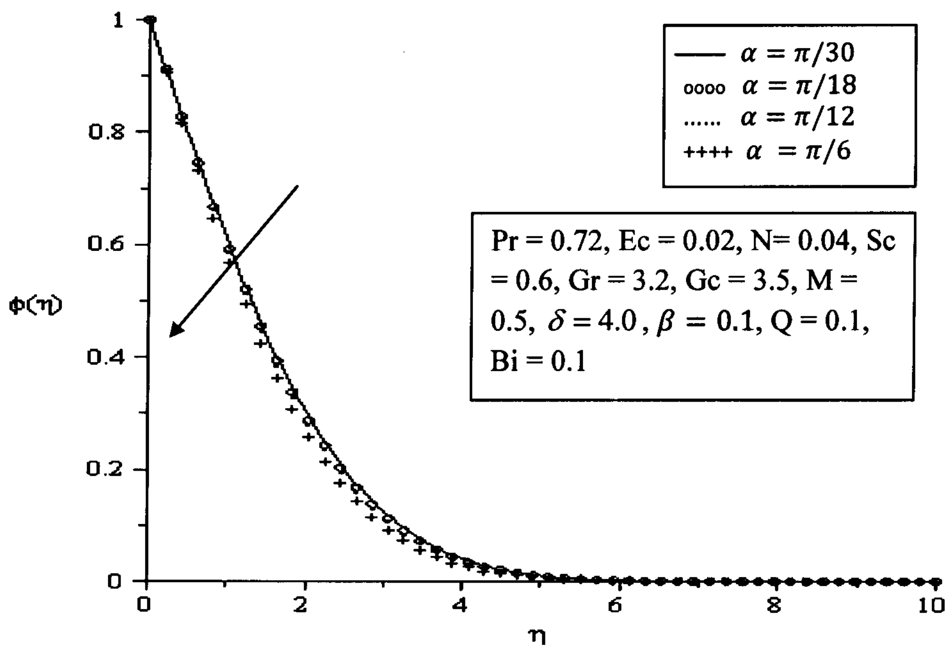

Figure 4.18: Effect of variation of angle of inclination on Concentration profile.

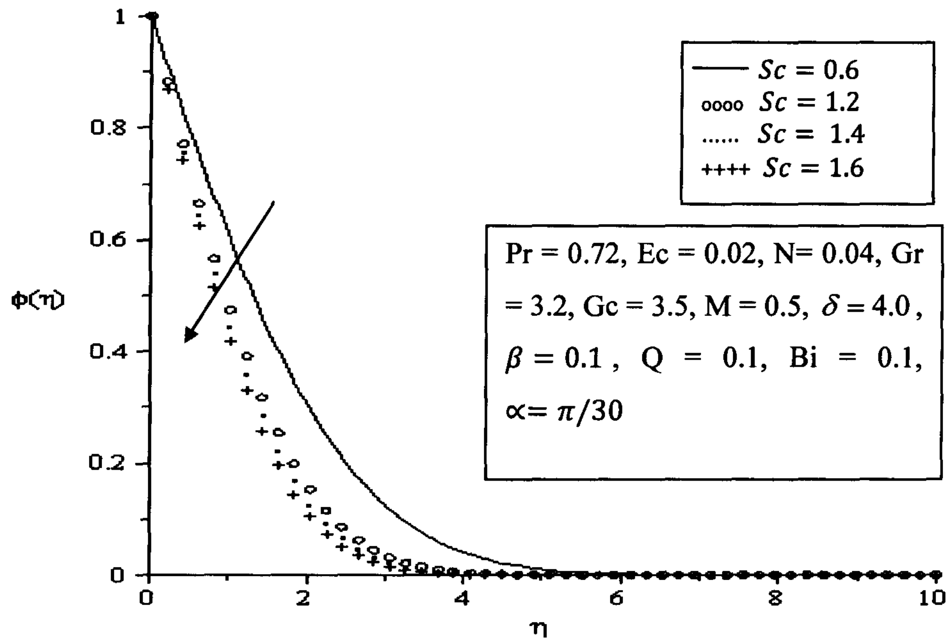

Figure 4.19: Effect of variation of Schmidt number on Concentration profile.

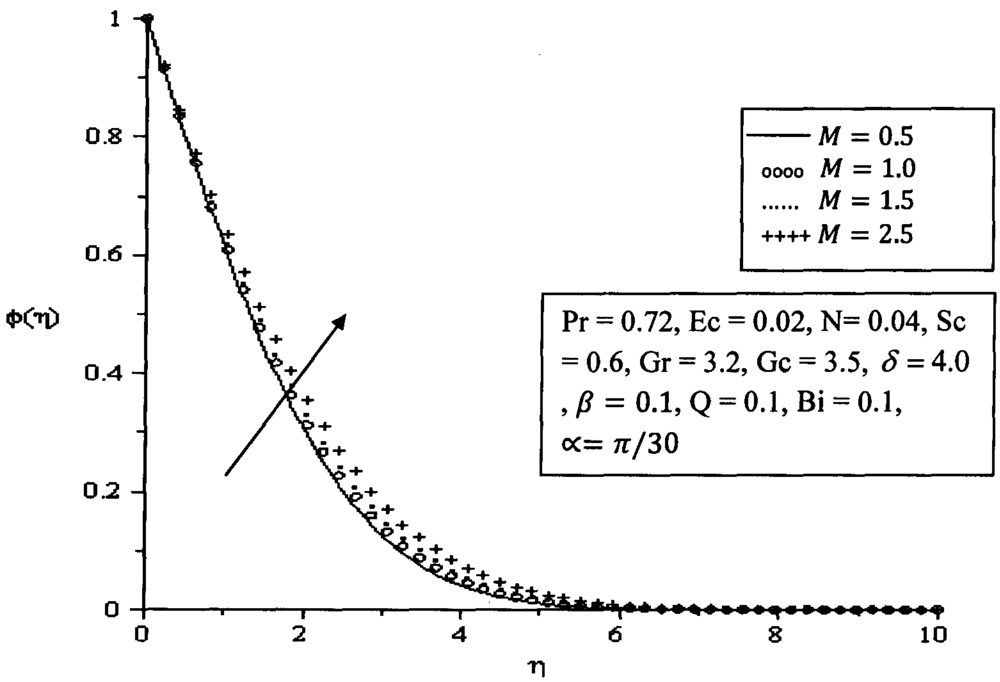

Figure 4.20: Effect of variation of Magnetic Parameter on Concentration profile.

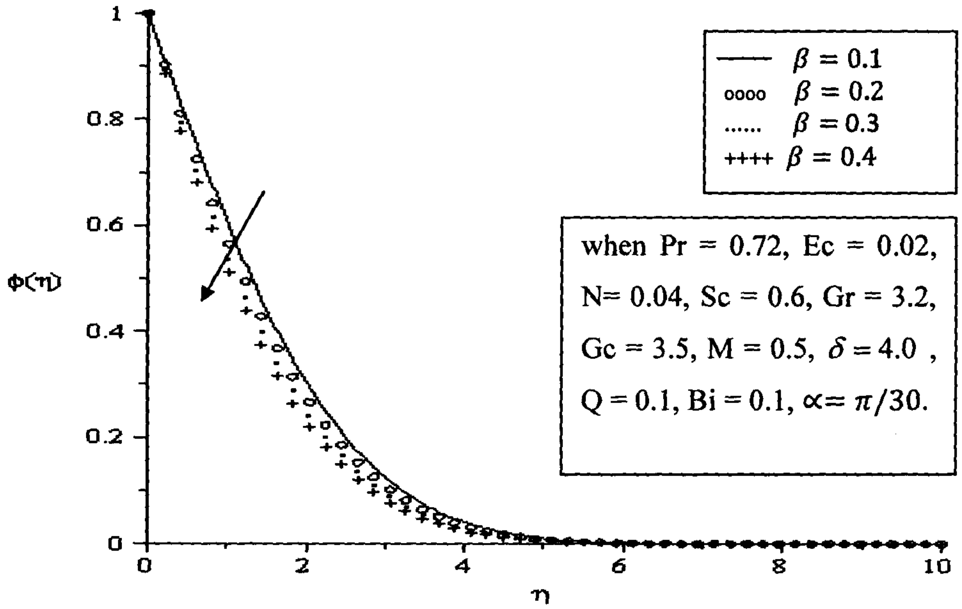

Figure 4.21: Effect of variation of Chemical Reaction Parameter on Concentration profile.

CHAPTER FIVE

5.0 CONCLUSIONS AND RECOMMENDATIONS

5.1 Introduction

In this chapter a summary of the effect of variation of parameters under study has been presented. Applications arising from the observed effects of some parameters have also been recommended for cooling and heating in industrial processes.

5.2 Conclusion

The study established that the orientation of a surface has effects on the heat and mass transfer characteristics. An increase in the angle of inclination increased the velocity of flow but decreased the temperature of the fluid within some ranges of inclination. The thermo-physical parameters were significant on the velocity, temperature and concentration profiles and the results are summarized as follows:

i. Velocity profiles significantly increased as the angle of inclination ($\propto$) increased. The velocity profiles were also observed to increase with viscous dissipation (N), thermal and Solutal Grashof numbers (Gr, Gc), Porosity(δ), Ecker number (Ec), Biot number (Bi) and local heat generation (Q) parameters. However, a decrease in velocity was also observed when the magnetic field parameter (M) and the Schmidt number were increased.

ii. The temperature decreased when the angle of inclination was within 0^o and 10^o or "cooling angle" and increased when the angle of inclination was greater than 10^o. The temperature also decreased when both thermal and solutal Grashof numbers (Gr and Gc respectively) were increased. However a rise in temperature was observed when the Prandtl number (Pr), Eckert number (Ec), Biot number (Bi), viscous dissipation parameter (N), Schmidt number (Sc) and local heat generation Parameter (Q) were increased.

iii. The concentration in the boundary layer decreases with increase in the angle of inclination($\propto$). A decrease in concentration was also observed when the chemical reaction paraeter (β), the Schmidt number (Sc), thermal Grashof number (Gr), solutal Grashof number (Gc) and Biot number (Bi) were increased. However an increase in concentration in the boundary layer was observed when the magnetic field parameter (M) was increased.

5.3 Recommendations

It is therefore recommended that;

i. In applying the technique of inclination to enhance cooling of material in industrial process the range of the "cooling angle" should be considered.

ii. The chemical reaction Parameter and Schmidt number which enhances mass diffusivity should be considered in processes involving fluid transportation.

iii. The viscous dissipation parameter had an integral effect in increasing the temperature in the boundary layer and should be considered in the design of heating systems.

iv. The study should be extended to nanofluid flow.

REFERENCES

Abdou, S. M.-K. (2007). Chemical reaction, heat, mass transfer on MHD flow over a vertical isothermal cone surface in micropolar fluids with heat generation/absorption. *Appl. Math. Sci-1, 34*, 1663-1674.

Ahmed, S. (2010). Free Convective Transient Three Dimensional Flow Through a Porous Medium Oscillating with time in the Presence of Peiodic Suction Velocity. *International Journal of Mathematics and Mechanics 6(11) Pp*, 1-16.

Aziz, A. (2009). A Similarity Solution for Laminar Thermal Boundary Layer Over a Flat Plate wiht a Convective Surface Boundary Conditiion. *Nonlinear Sci. Num. simul. 14 Pp.* , 1064-1068.

Beg O. A, B. T. (2009). Chemically Reacting Mixed Convective Heat and Mass Transfer along Inclined and vertical Plates with soret and Dufour Effects: Numerical Solutions. *International Journal of Applied Mathematics and Mechanics 5(2), Pp*, 39-57.

Blasius, H. (1908). Grenzschichten in flussifkeiten mit kleineer reibung. *Z Math Phys 56*, 1.

Cortell, R. (2005). Numerical solutions of the classical blasius flat plate problem. *Appliend Mathematics and Computation 170*, 706.

Cortell, R. (2008). A numerical tackling on sakiadis flow with thermal radiation. *Chinese Physics Letters 25*, 1340.

Crane, L. J. (1970). Flow Past the Stretching Plate. *Z Angew Math Phys 21*, 645.

Das, G. C. (2010). Effect of chemical reaction on free convection flow through a porous medium bounded by a vertical surface. *J.Eng.Phy& Them Phy.,83,No-1*, 130-140.

Etwire, C. J., & Seini, Y. I. (2014). Radiative MHD Flow over a Vertical Plate with Convective Boundary Condition. *American J. of Appl. Math. Vol. 2, No. 6, Pp.* , 214-220.

Falkner, V. M., & Skan, S. W. (1931). Some Approximate Solutions of th boundary layer Equations. *Phil Mag 12*, 865.

Gebharat, B. (1962). Effects of Viscous Dissipation in External Natural Convection Flows. *J. of Fluid Mech. 38, Pp.* , 97-107.

Gnaneswara, R. M., & Bhaskar, R. N. (2011). Mass Transfer and Heat Generation Effects on Mhd Free Convection Flow Past an Inclined Vertical Surface in a Porous Medium. *Journal of Applied Fluid Mechanics, 4(3), Pp.* , 7-11.

Gnaneswara, R. M., & Bhaskar, R. N. (2011). Radiation and Mass Transfer Effects on Unsteady MHD Free Convection Flow Past a Semi-infinite Moving Vertical Plate in a Porous Medium with viscous Dissipation. *Int. J. Appl. Math and Mech 6(1) Pp.*, 1-12.

Hossain, M. M., & Mojumder, R. (2010). Similarity Solution for Steady Natural Convection Boundary Layer Flow and Heat Transfer above a Heated Horizontal Surface with Transpiration. *Int. J. of Appl. Math. and Mech. Vol. 6. Number 4, Pp.*, 1-16.

Ibrahim, F. S., Elaiw, A. M., & Bak, A. A. (2008). Effect of chemical reaction and radiation absorption on the unsteady MHD free convection flow past a semi infinite vertical permeable moving plate with heat source and suction. *Comm In Nonlinear Sc. Num. Simulation Vol. 13*, 1056-1066.

Ibrahim, S. Y., & Makinde, O. D. (2010). Chemically reacting MHD boundary layer flow of heat and mass transfer over a moving vertical plate with suction. *Scientific Research and Essays Vol. 5(19)*, 2875-2882.

Ibrahim, S. Y., & Makinde, O. D. (2011). Chemically Reacting Magnetohydrodynamics (MHD) Boundary Layer Flow of Heat and Mass Transfer past a Low-Heat-Resistant Sheet Moving Vertically Downwards. *Scientific Research and Essays, Vol 6(22) Pp.*, 4762-4775.

Kandasamy, R. (2005). Chemical reaction, heat and mass transfer on MHD flow over a vertical moving surface with heat source and thermal stratification effects. *International journal of heat and mass transfer, 48*, 4554-4561.

Makinde, O. D. (2007). Domain Decomposition Approach to a Boundary Layer Flow with Thermal Radiation Past a Moving Vertical Porous Plate. *International Journal of Applied Mathematics and Mechanics, 3(3) Pp.*, 62-70.

Makinde, O. D. (2010). On MHD heat and Mass Transfer Over a Moving vertical Plate with a Convective Surface Boundary Conditon. *Canadian Journal of Chemical Engineering, Vol. 88, no 6, PP.*, 983-990.

Makinde, O. D., & Olanrewaju, P. O. (2010). Bouyancy Effects on Thermal Boundary Layer Over a Vertical Plate with Convective Surface Boundary Condition. *J. of Fluids Engineering* , Vol. 132/044502-1.

Mansour, M. A., Mohammed, R. A., Abd-Elaziz, M. M., & Ahmed, S. E. (2007). Fluctuating Thermal Diffusion on Unsteady MHD Convection of Micropolar Fluid through a Porous Medium past a vertical Plate in Slip-Flow Regime. *International Journal of Applied Mathematics and Mechanics, 3(3), Pp.*, 99-117.

Muthucumaraswamy, R. (2002). Effects of chemical reaction on a moving isothermal vertical surface with suction. *Acta Mech, 155*, 65-70.

Muthucumaraswamy, R., & Janakiraman, B. (2008). Mass transfer effects on isothermal vertical oscilating plate in presence of chemical reactions,. *Int. J. of Appl. Math. and Mech. 4(1)*, 66-74.

Prandtl, L. (1904). Uberr flussigkeitsbewegungen bei sehr kleiner reibung. *Intem Math Kongr Heidelberg*, 484.

Reddy, M. G., & Reddy, N. B. (2010). Soret and Dufoure Effects on Steady MHD Free Convection Flow Past a Semi-infinite Moving Vertical Plate in a Porous Medium with Viscous Dissipation. . *International Journal of Applied Mathematics and Mechanics. 6(1), Pp.*, 1-12.

Sakiadis, B. C. (1961). Boundary layer behaviour on Continuous Solid surface. *J AlChe*, 7:26.

Seini, Y. I. (2013). Flow over Unsteady Stretching Surface with Chemical Reaction and Non-uniform Heat Source. *Journal of Engineering and Manufacturing Technology, JEMT 1 (2013)*, 24-35.

Senapati, N., Dahal, R. K., & Das, T. K. (2012). Effects of Chemical Reaction on Free Convection MHD Flow through Porous Medium Bounded by Vertical Surface with Slip Flow Region. *American Journal of Computational and Applied Mathematics,2(3d)*, 124-135.

Shit, G. C. (2009). Hall Effects On MHD Free Convective Flow and Mass Transfer Over a Stretching Sheet. *International Journal of Applied Mathematics and Mechanics, 5(8), Pp*, 23-38.

Sivasankaran, S., Bhuvaneswar, M., Kandaswamy, P., & Ramasami, E. K. (2006). Lie Group Analysis of Natural Convection Heat and Mass Transfer in an Inclined Surface. *Nonlinear Analysis: Modeling and Control, 11(1), Pp.*, 201-212.

APPENDICES

APPENDIX A: Publications.

C.J. Etwire, Y.I. Seini, **D.A. Azure (2015)**, MHD Thermal Boundary Layer Flows over a Flat Plate with Internal Heat Generation, Viscous Dissipation and Convective Surface Boundary Conditions. Intl. J. Emerging Tech. and Advance Eng, 5 (5), 335-342.

APPENDIX B: Maple numerical code for solving the system of ordinary differential equations.

$> \; Pr := 0.72 : M := 0.5 : \beta := 0.1 : Gc := 3.5 : Gr := 3.2 : \alpha := \frac{\pi}{30} :$
$Sc := 0.6 : Q := 0.1 : Ec := 0.02 : N := 0.04 : \delta := 4 : Bi := 0.1$

$fcns := \{F(y), \theta(y), \phi(y)\} :$

$sys := diff(F(y), y\$3) + \frac{1}{2} \cdot F(y) \cdot diff(F(y), y\$2) + Gr \cdot \theta(y) \cdot \sin(\alpha) + Gc \cdot \phi(y) \cdot \sin(\alpha) - (\delta + M) \cdot diff(F(y), y) + \delta = 0, diff(\theta(y), y\$2) + \frac{1}{2} \cdot Pr \cdot F(y) \cdot diff(\theta(y), y) + Ec \cdot Pr \cdot (diff(F(y), y\$2))^2 + N \cdot Pr \cdot (diff(F(y), y))^2 + Pr \cdot Ec \cdot M \cdot (diff(F(y), y)) + Q \cdot Pr \cdot \theta(y) = 0, diff(\phi(y), y\$2) + \frac{1}{2} \cdot Sc \cdot F(y) \cdot diff(\phi(y), y) - Sc \cdot \beta \cdot \phi(y) = 0, D(F)(0) = 0, F(0) = 0, D(\theta)(0) = Bi \cdot ((\theta)(0) - 1), \phi(0) = 1, D(F)(10) = 1, \theta(10) = 0, \phi(10) = 0 :$

$$\frac{d^3}{dy^3} F(y) + \frac{1}{2} F(y) \left(\frac{d^2}{dy^2} F(y) \right) + 3.2\, \theta(y) \sin\left(\frac{1}{30} \pi \right) + 3.5\, \phi(y) \sin\left(\frac{1}{30} \pi \right) - 4.5 \left(\frac{d}{dy} F(y) \right) + 4 = 0, \frac{d^2}{dy^2} \theta(y) + 0.3600000000 F(y) \left(\frac{d}{dy} \theta(y) \right) + 0.0144 \left(\frac{d^2}{dy^2} F(y) \right)^2 + 0.0288 \left(\frac{d}{dy} F(y) \right)^2 + 0.00720 \left(\frac{d}{dy} F(y) \right) + 0.072\, \theta(y) = 0, \frac{d^2}{dy^2} \phi(y) + 0.3000000000 F(y) \left(\frac{d}{dy} \phi(y) \right) - 0.06\, \phi(y) = 0, D(F)(0) = 0, F(0) = 0, D(\theta)(0) = 0.1\, \theta(0) - 0.1, \phi(0) = 1, D(F)(10) = 1, \theta(10) = 0, \phi(10) = 0$$

$p := dsolve(\{sys, D(F)(0) = 0, F(0) = 0, D(\theta)(0) = Bi \cdot ((\theta)(0) - 1), \phi(0) = 1, D(F)(10) = 1, \theta(10) = 0, \phi(10) = 0\}, fcns, type = numeric, method = bvp, abserr = 1e-6)$

proc(x_bvp) ... **end proc**

$dsol1 := dsolve(\{sys\}, numeric, output = operator)$

$[y = \mathbf{proc}(y)\ \dots\ \mathbf{end\ proc}, F = \mathbf{proc}(y)\ \dots\ \mathbf{end\ proc}, \mathrm{D}(F) =$
$\mathbf{proc}(y)$
...
$\mathbf{end\ proc}, \mathrm{D}^{(2)}(F) = \mathbf{proc}(y)\ \dots\ \mathbf{end\ proc}, \phi = \mathbf{proc}(y)$
...
$\mathbf{end\ proc}, \mathrm{D}(\phi) = \mathbf{proc}(y)\ \dots\ \mathbf{end\ proc}, \theta = \mathbf{proc}(y)\ \dots\ \mathbf{end\ proc},$
$\mathrm{D}(\theta) = \mathbf{proc}(y)\ \dots\ \mathbf{end\ proc}]$

dsol1(0);

$[y = 0, F(0) = 0., \mathrm{D}(F)(0) = 0., \mathrm{D}^{(2)}(F)(0) = 2.119394378828209033,$
$\phi(0) = 0.99999999999999978, \mathrm{D}(\phi)(0) =$
$-0.429001727908662478, \theta(0) = 0.515880212934890392, \mathrm{D}(\theta)(0)$
$= -0.0484119787065109553]$

APPENDIX C: Numerical Formulae for Solving the System of Ordinary Differential Equations.

i. The Fourth order Runge-Kutta Formula.

$$k_1 = hf(x_n, y_n)$$

$$k_2 = hf\left(x_n + \frac{h}{2}, y_n + \frac{k_1}{2}\right)$$

$$k_3 = hf\left(x_n + \frac{h}{2}, y_n + \frac{k_2}{2}\right)$$

$$k_4 = hf\left(x_n + h, y_n + k_3\right)$$

$$y_{n+1} = y_n + \frac{k_1}{6} + \frac{k_2}{3} + \frac{k_3}{3} + \frac{k_4}{6} + O(h^5)$$

Where h is the step size.

ii. The Newton-Raphson's formula.

$$x_1 = x_o - \frac{f(x_o)}{f'(x_0)}$$

$$x_{i+1} = x_i - \frac{f(x_i)}{f'(x_i)}$$

Where x_o is an initial guess.